Fundamental and applied aspects of high energy particle interaction with oriented crystals

Viktor V. Tikhomirov Institute for Nuclear Problems, Belarusian State University, Minsk, Belarus

August 17, 2018 XIV Gomel School

Plan

Intoduction.

– *Crystal field strength and particle motion variety*

– *Synchrotron type radiation and pair production investigation in 80-th*

Present joint investigations of high-energy electron radiation in crystals with Ferrara group at CERN and MAMI

– *simulation methods*

– *radiation at multiple volume reflection*

– *electromagnetic showers in **PWO***

– *"positron source" (radiation in **W**)*

– gamma-telescopes, *polarization effect. The most precise experiment* in *Nature*

The uniqueness of crystal field

Moving in oriented crystals, particles come under the action of the practically inter-atomic-scale ***effective crystal field***

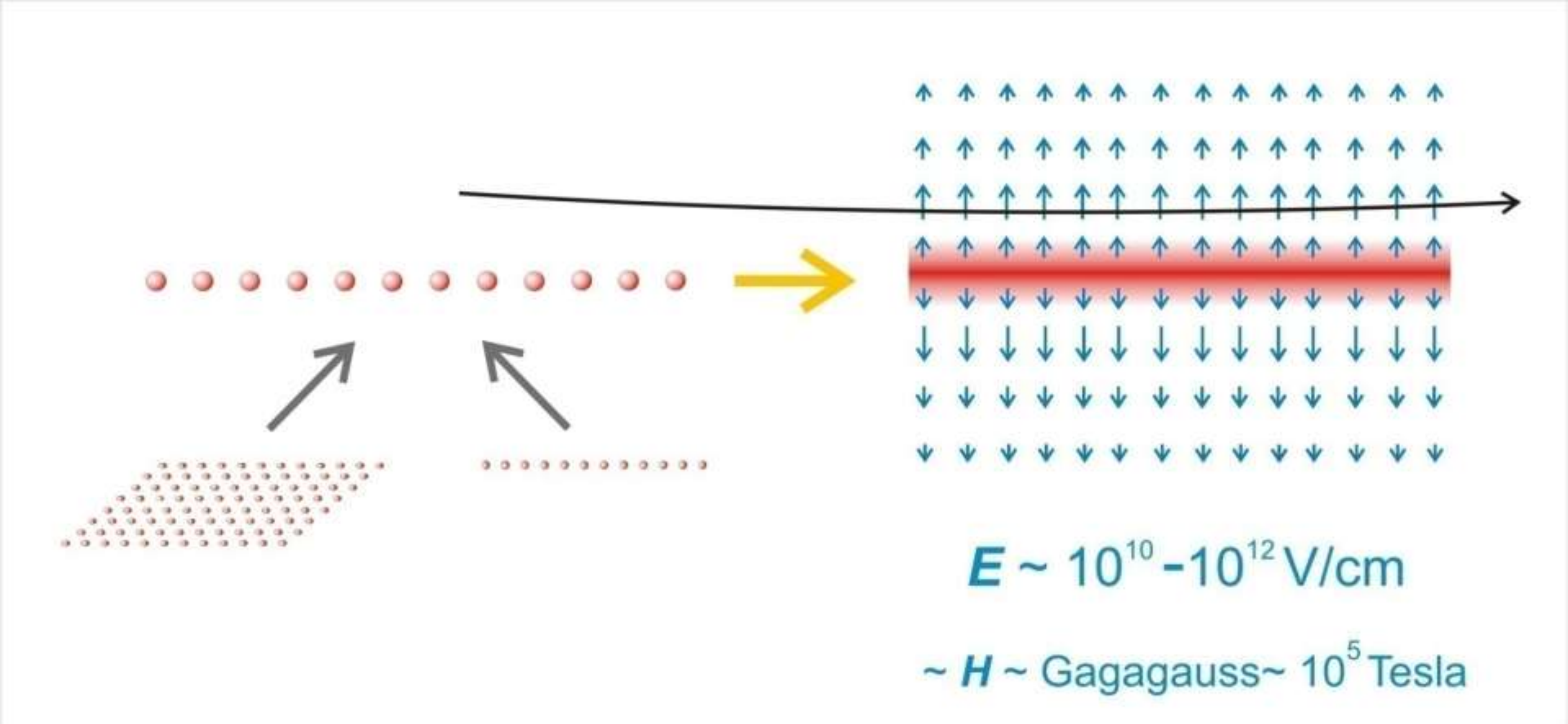

Simulated situations

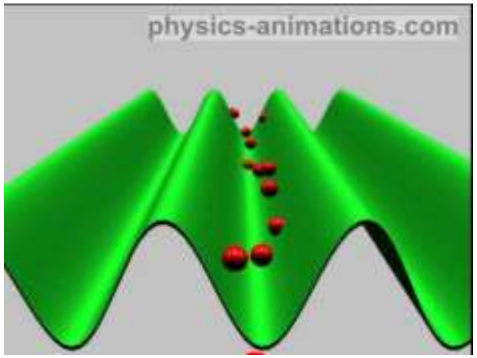

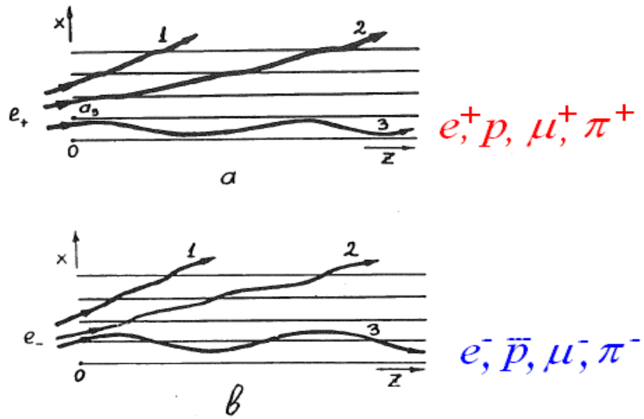

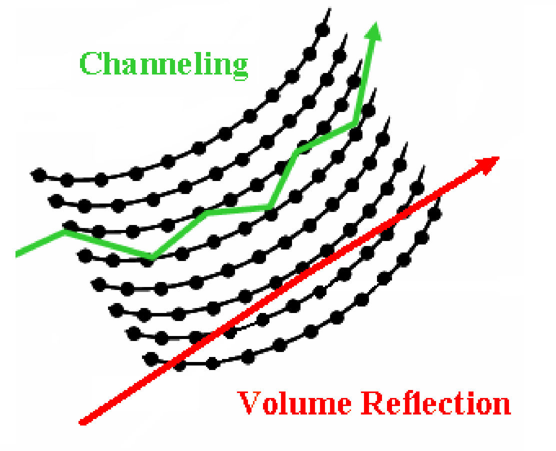

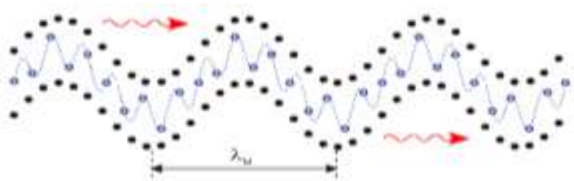

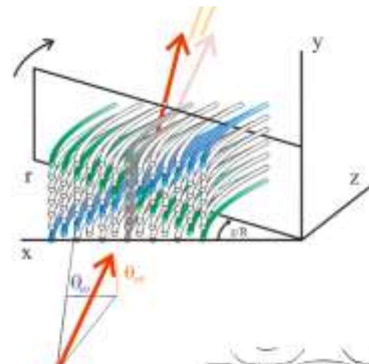

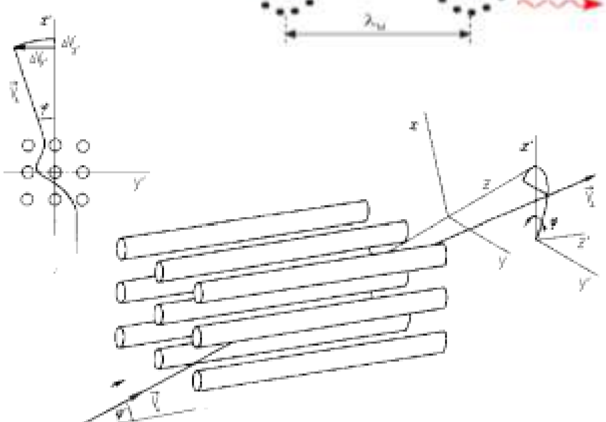

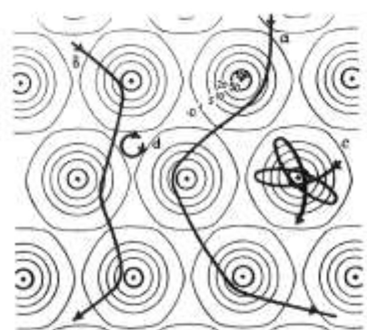

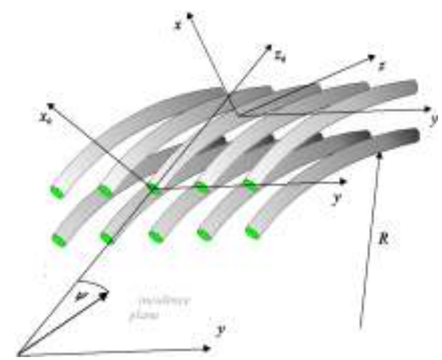

Critical electron and photon energies

Baryshevsky, Tikhomirov UFN, 1989

element	Z	*plane / axis*	$E_{\mathbf{max}}$ (GV/cm)	**H_{eff} (kilotesla)**	**$\hbar\omega_{cr} = \varepsilon_{cr}$ (GeV)**
Si	14	*plane* (110)	5.7	**1.9**	**1200**
Ge	32	*axis* ‹110›100K	144	**48**	**47**
W	74	*axis* ‹111›	500	**167**	**13.6**

Crystals are a key ingredient for the final stages of both routes (linear and circular) to 1 **PeV** collisions.

F. Zimmermann

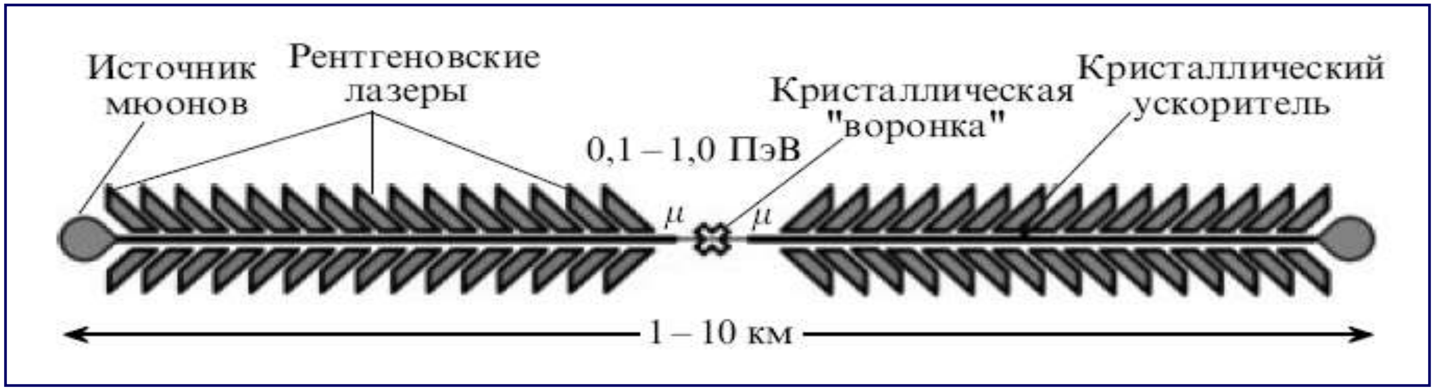

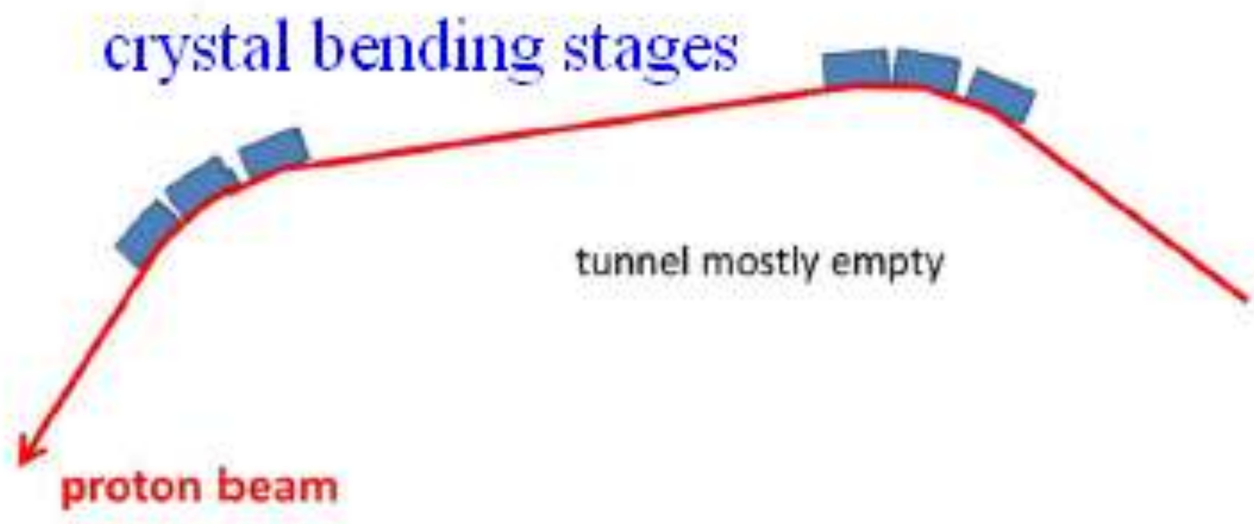

Critical electric field

$$E_0 = \frac{m^2 c^3}{e\hbar} \approx 1.32 \times 10^{16}\, eV$$

produces the work mc^2

on the Compton wavelength $\lambda\!\!\!^{-} = \frac{\hbar}{mc}$:

$$eE_0 \lambda\!\!\!^{-} = e\frac{m^2 c^3}{e\hbar}\frac{\hbar}{mc} = mc^2$$

A virtual pair conversion to a real one in electric field $E \sim E_0$

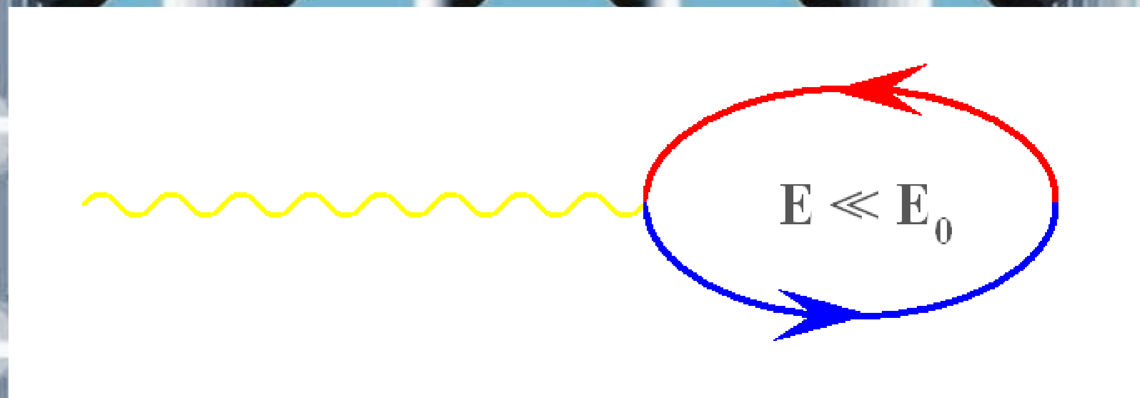

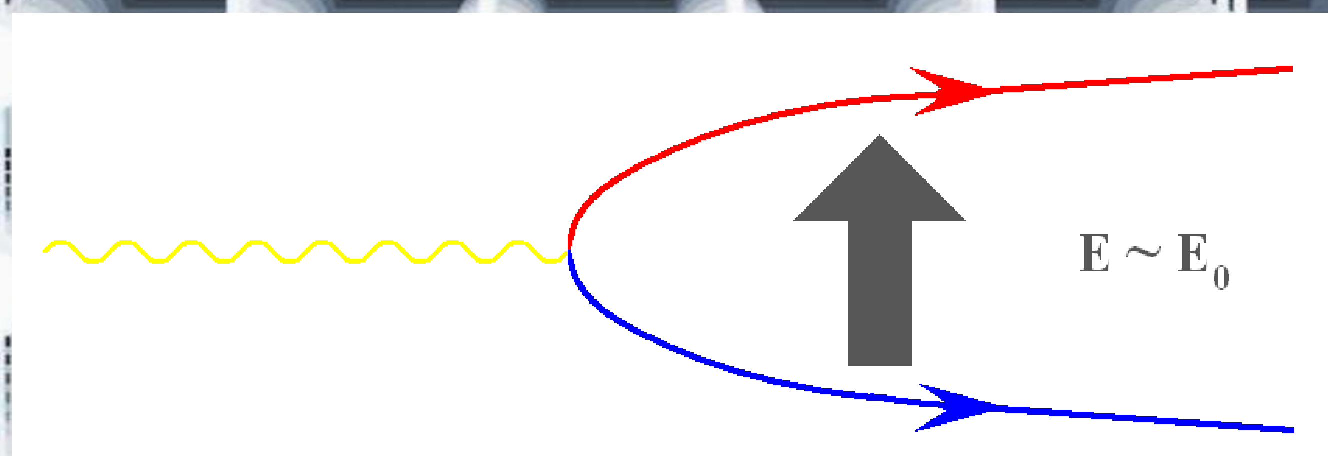

Critical electron and photon energies

Baryshevsky, Tikhomirov UFN, 1989

element	Z	*plane / axis*	$E_{\mathbf{max}}$ (GV/cm)	$\mathbf{H_{eff}}$ **(kilotesla)**	$\hbar\omega_{cr} = \varepsilon_{cr}$ **(GeV)**
Si	14	*plane* (110)	5.7	**1.9**	**1200**
Ge	32	*axis* ‹110›100K	144	**48**	**47**
W	74	*axis* ‹111›	500	**167**	**13.6**

Ноябрь 1989 г. *Том 159, вып. 3*

УСПЕХИ ФИЗИЧЕСКИХ НАУК

ИЗ ТЕКУЩЕЙ ЛИТЕРАТУРЫ

539.12

РАДИАЦИОННЫЕ ПРОЦЕССЫ МАГНИТОТОРМОЗНОГО ТИПА В КРИСТАЛЛАХ И СОПРОВОЖДАЮЩИЕ ИХ ПОЛЯРИЗАЦИОННЫЕ ЯВЛЕНИЯ

В. Г. Барышевский, В. В. Тихомиров

(Институт ядерных проблем
при Белорусском государственном университете им. В. И. Ленина)

СОДЕРЖАНИЕ

Предсказание магнитотормозного ОП в кристаллах

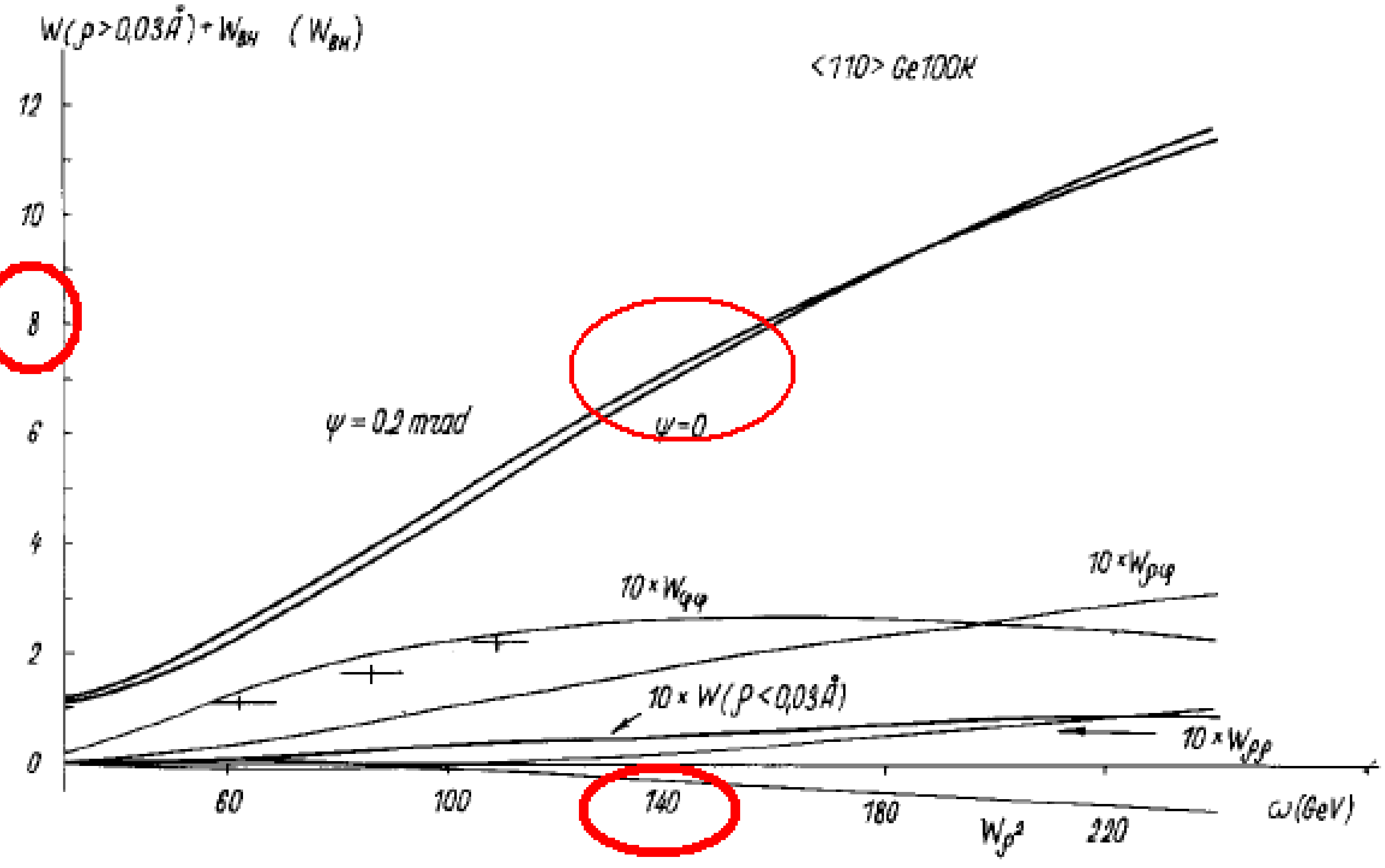

В.Г. Барышевский, В.В. Тихомиров 1982-1985 гг.

Наблюдение: of the 8-time increase of PP probability in Ge<110> 100K at 150 GeV

A. Belkacem, PRL 1987

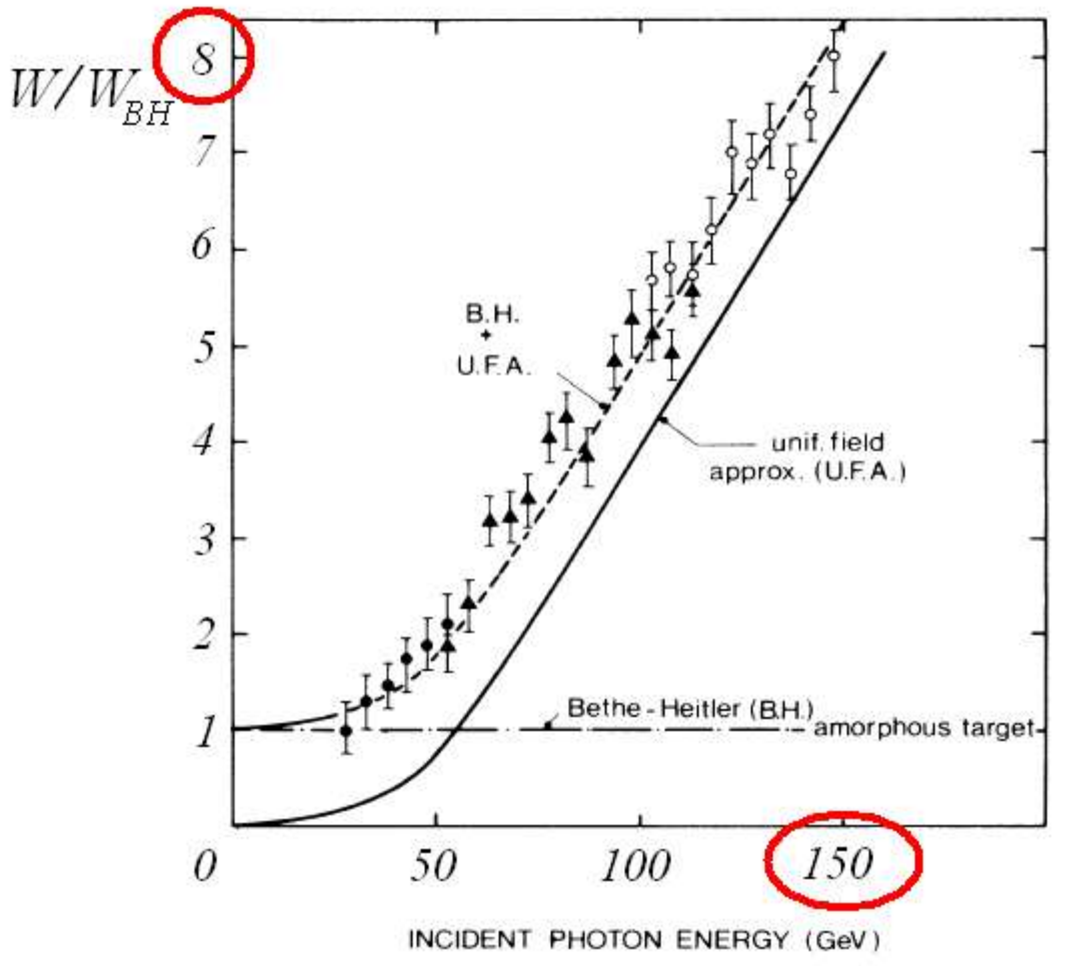

25/14-time increase of radiative energy losses of 150 GeV electrons in 0.4/1.4 mm Ge<110> 100K

A. Belkacem, PRL 1985

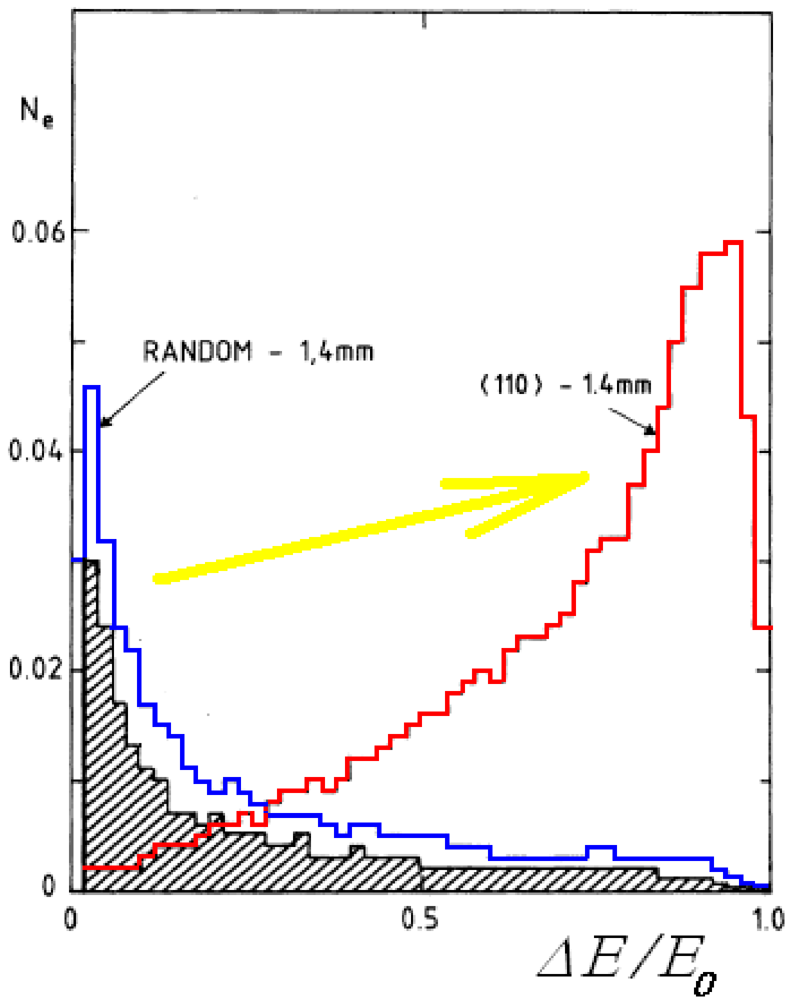

Electron radiative cooling (150 GeV e^- 185 μm Ge<110> 100K)

Baryshevskii V. G., Dubovskaya I. Ya. // Phys. Lett. 1977. Vol. A62. P. 45.

Belkacem A. et al. // Phys. Lett. 1986. Vol. B177. P. 211.

Tikhomirov V. V. // Phys. Lett. 1987. Vol. A125. P. 411.

Tikhomirov V. V. // Nucl. Instr. Meth. 1989. Vol. B36. P. 282.

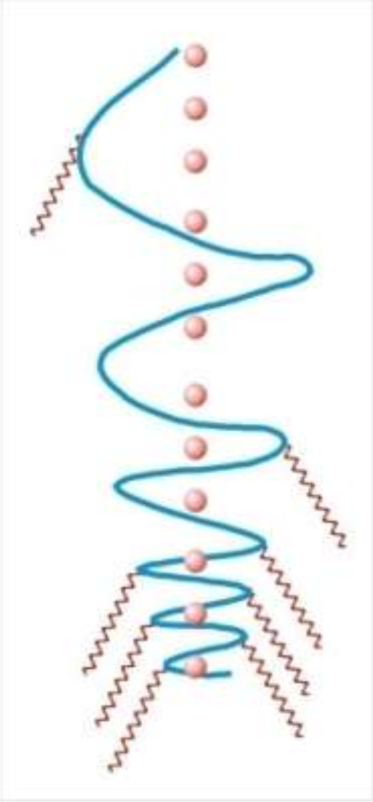

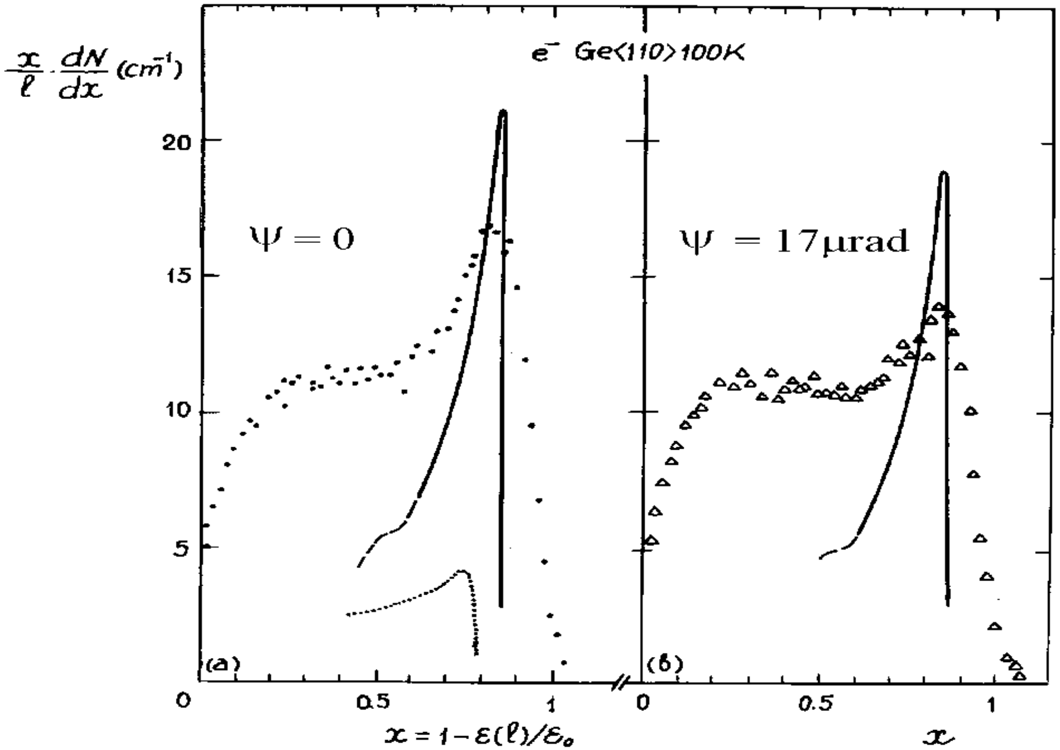

General simulation method

Incoherent scattering in crystals

Presently used:

Kitagawa-Ohtsuki approximation

$$\left\langle \frac{\Delta p_\perp^2}{\Delta z} \right\rangle \cong P(r_\perp) \times \left\langle \frac{\Delta p_\perp^2}{\Delta z} \right\rangle_{\text{random}}$$

$$P(r_\perp) = \frac{r_0^2}{\rho_\perp^2} \exp\left(-\frac{r_\perp^2}{\rho_\perp^2}\right), \qquad P(y) = \frac{d_y}{(2\pi)^{1/2}\rho_y} \exp\left(-\frac{y^2}{2\rho_y^2}\right).$$

+ *suppression by coherent scattering*

$$\langle d\vartheta_s^2(z)/dz \rangle = n \int_0^{\vartheta_2} \int_0^{2\pi} \vartheta^2 \frac{d\sigma}{d\Omega} [1 - \underline{\exp(-p^2\vartheta^2 u_1^2)}] d\varphi \vartheta d\vartheta$$

This approach is equivalent to the

plane wave approximation

and does not take into consideration

both **particle and nuclei**

transverse distribution **nonuniformity** is classical formula

$$\theta(\mathbf{r}) = \frac{2Ze^2}{pva}\sum_{i=1}^{3}\alpha_i\beta_i K_1(\beta_i \mathbf{r}/a)$$

applicable for relativistic elementary particles?

– no, it is not!

§126. The quasi-classical case

It is of interest to investigate the manner in which the passage occurs from the quantum-mechanical theory of scattering to the limit of the classical theory.

If we can speak of classical scattering through an angle θ when the particle is incident at an impact parameter ρ, it is necessary that the quantum-mechanical indeterminacies of these two quantities should be relatively small: $\Delta\rho \ll \rho$, $\Delta\theta \ll \theta$. The indeterminacy in the scattering angle is of the order of magnitude $\Delta\theta \sim \Delta p/p$, where p is the momentum of the particle and Δp is the indeterminacy in its transverse component. Since $\Delta p \sim \hbar/\Delta\rho \gg \hbar/\rho$, we have $\Delta\theta \gg \hbar/p\rho$, and thus

$$\theta \gg \hbar/\rho m v. \tag{126.6}$$

The classical angle of deviation of the particle can be estimated as the ratio of the transverse momentum increment Δp during the "collision time" $\tau \sim \rho/v$ and the original momentum mv. The force acting on the particle at a distance ρ is $U'(\rho)$; hence $\Delta p \sim |U'(\rho)|\rho/v$, so that $\theta \sim |U'(\rho)|\rho/mv^2$.

Substitution in (126.6) gives the condition for quasi-classical scattering in the form

$$|U'(\rho)|\rho^2 \gg \hbar v. \tag{126.7}$$

The classical angle of deviation of the particle can be estimated as the ratio of the transverse momentum increment Δp during the "collision time" $\tau \sim \rho/v$ and the original momentum mv. The force acting on the particle at a distance ρ is $U'(\rho)$; hence $\Delta p \sim |U'(\rho)|\rho/v$, so that $\theta \sim |U'(\rho)|\rho/mv^2$.

Substitution in (126.6) gives the condition for quasi-classical scattering in the form

$$|U'(\rho)|\rho^2 \gg \hbar v. \qquad (126.7)$$

For a Coulomb field, $U = \alpha/r$, the condition (126.7) is satisfied if $\alpha \gg \hbar v$. This is the opposite condition to that for which the Coulomb field can be regarded as a perturbation. We shall see, however, that the quantum theory of scattering in a Coulomb field leads to a result which, as it happens, is always in agreement with the classical result.

Since $\dfrac{Z\alpha}{\beta} \approx \dfrac{14}{137} \ll 1$ **the single-atom scattering is "quantum" and can be treated as a perturbation**

classical *vs* quantum scattering

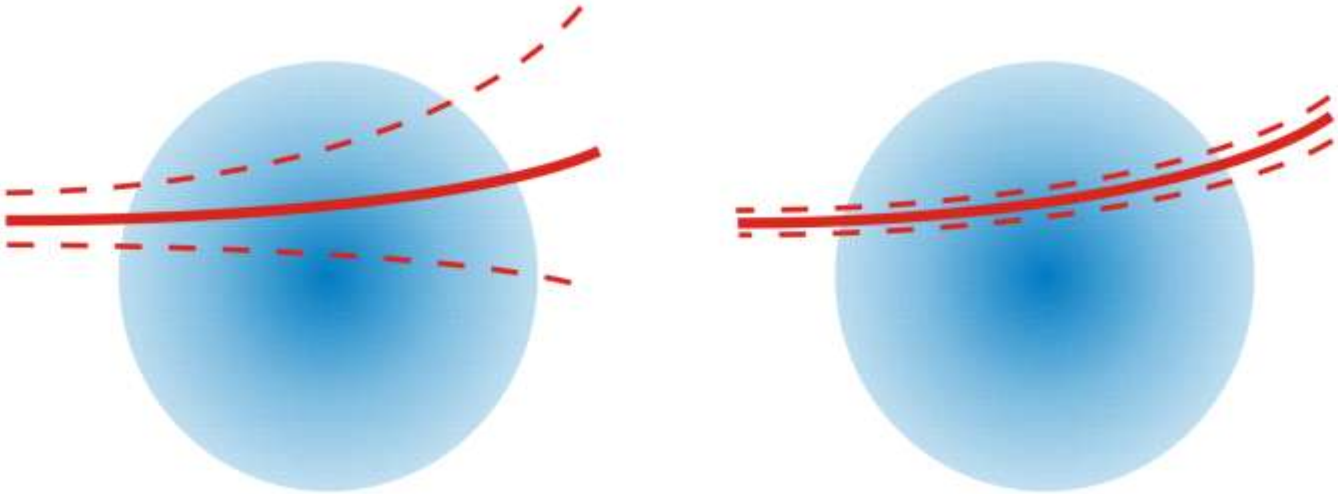

$$\frac{Z\alpha}{\beta} \ll 1$$

quantum

$$\frac{Z\alpha}{\beta} \gg 1$$

classical

Further refinement

of incoherent scattering

quantum theory in crystals

Incoherent scattering in the presence of coherent one (Wigner function + Born approximation)

$$\Delta\psi + p^2\psi = 2\varepsilon\left[U(x) + \delta U(\vec{r})\right]\psi,$$

$$\psi \approx \exp\left(ipz' - i\int U(\vec{\rho}', z')\frac{dz'}{v}\right)\left[1 - i\int \delta U(\vec{\rho}', z')\frac{dz'}{v}\right],$$

$$P(\vec{\rho}', \vec{q}) = \frac{1}{\pi^2}\int \psi^*(\vec{\rho}' + \vec{\chi})\psi(\vec{\rho}' - \vec{\chi})\exp(2i\vec{q}\,\vec{\chi})d^2\chi$$

$$P(\vec{\rho}', \vec{q}) = \frac{1}{\pi}\delta(q_y)\int \exp\left(i\int\left[U(x' + \chi_{x'}, z) - U(x' - \chi_{x'}, z)\right]\frac{dz'}{v}\right)\exp(2iq_{x'}\chi_{x'})d\chi_{x'} \approx$$

$$\approx \frac{\delta(q_{y'})}{\sqrt{\pi\left|\int U''dz'/v\right|}}\exp\left\{i\left[\frac{\pi}{4}\operatorname{sgn}\left(\int U''dz'/v\right) - \frac{\left(q_{x'} + \int U'dz'/v\right)^2}{\int U''dz'/v}\right]\right\} \to \delta(q_y)\delta\left(q_{x'} + \int U'(x)\frac{dz}{v}\right),$$

Trajectories

are simulated classically

at nigh (>> 100 MeV) energies

Some trajectories

In transverse plain

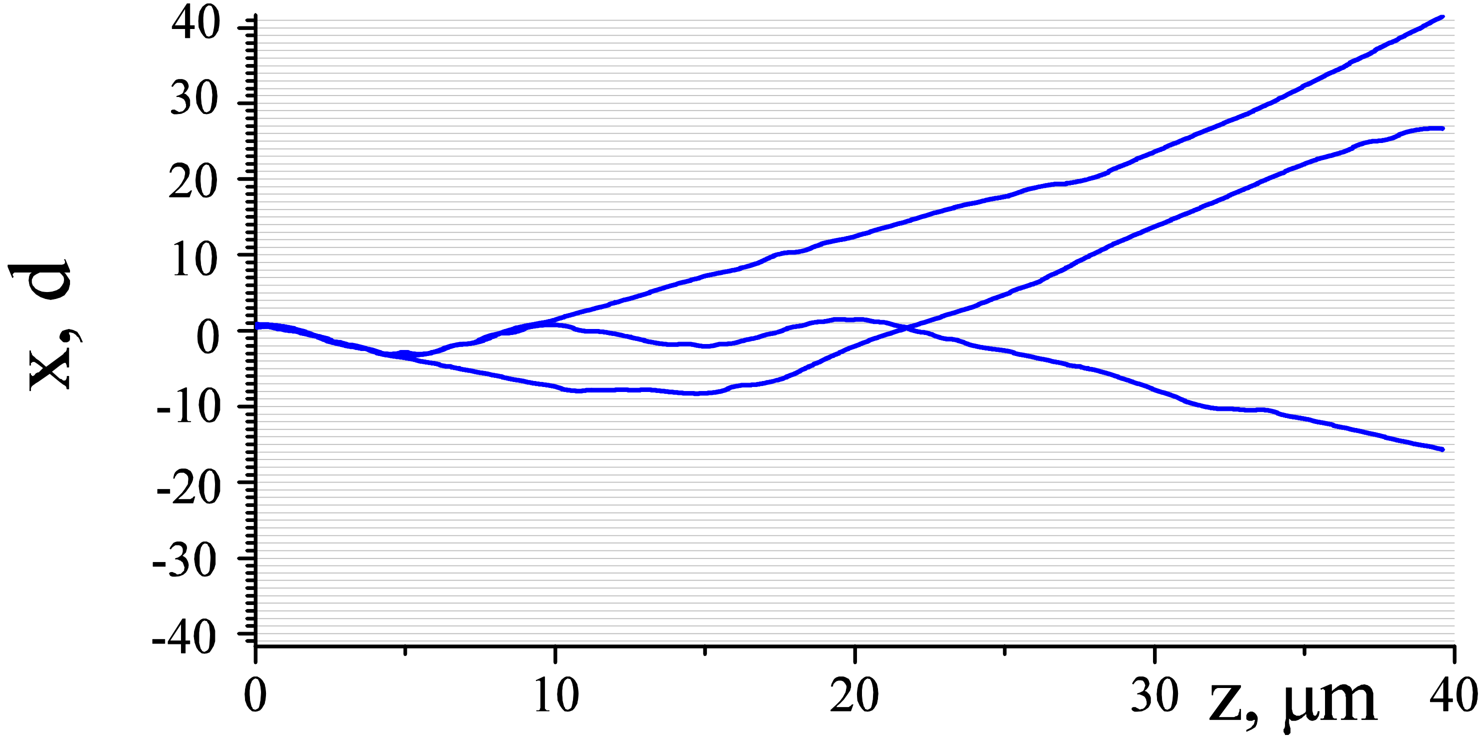

Траектории электронов с энергией 855 МэВ в кристалле, использованном для изготовления ондулятора в эксперименте на MAMI

Backe H., et al. Nuov. Cim. 2011. V. 34 C. P. 157.

Backe H., et al. Nucl. Instrum. Methods Phys. Res. 2013. V. B 309. P. 37.

Горизонтальные линии изображают кристаллические плоскости (110), расположенные на расстоянии 0.192 нм.

A “*fortunate*” 500 MeV positron trajectory

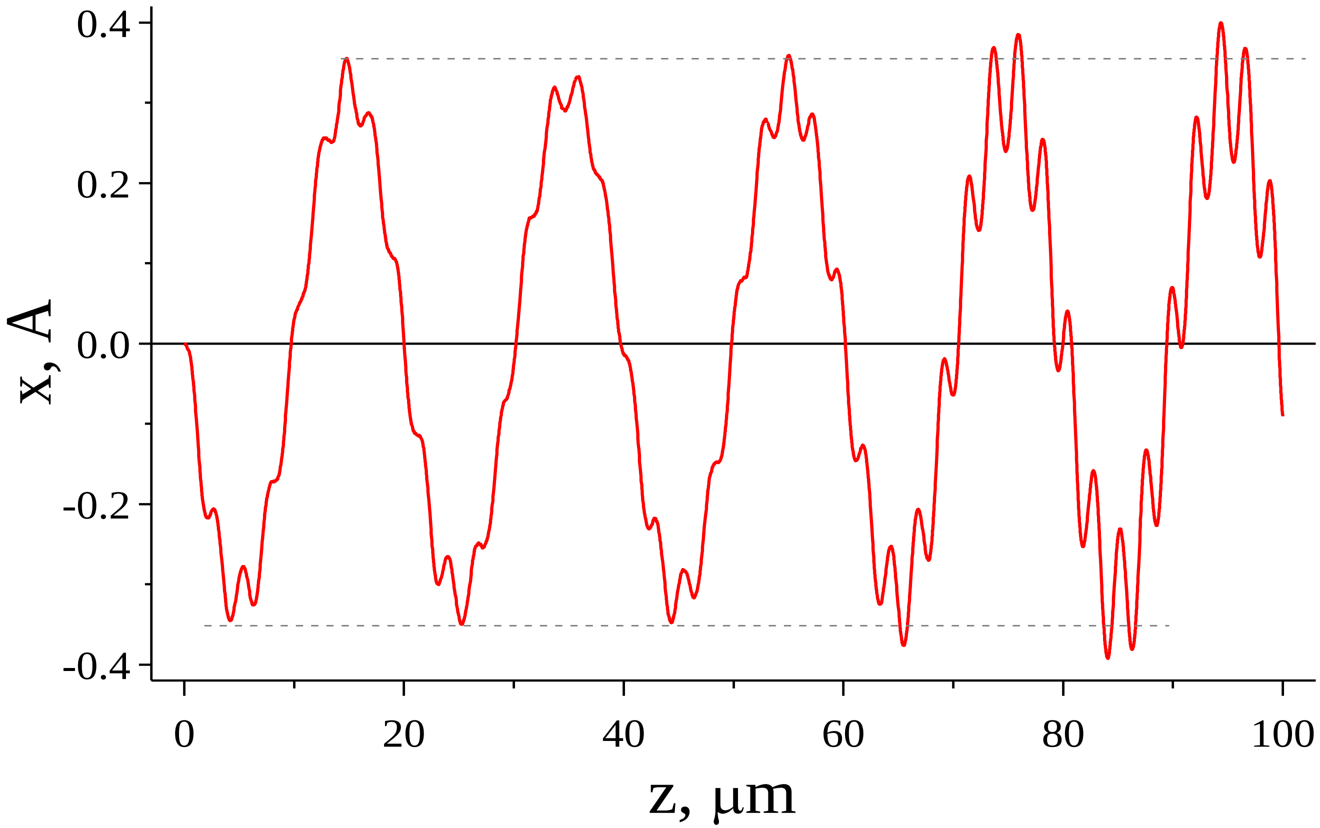

Simultaneous doughnut scattering and MVR

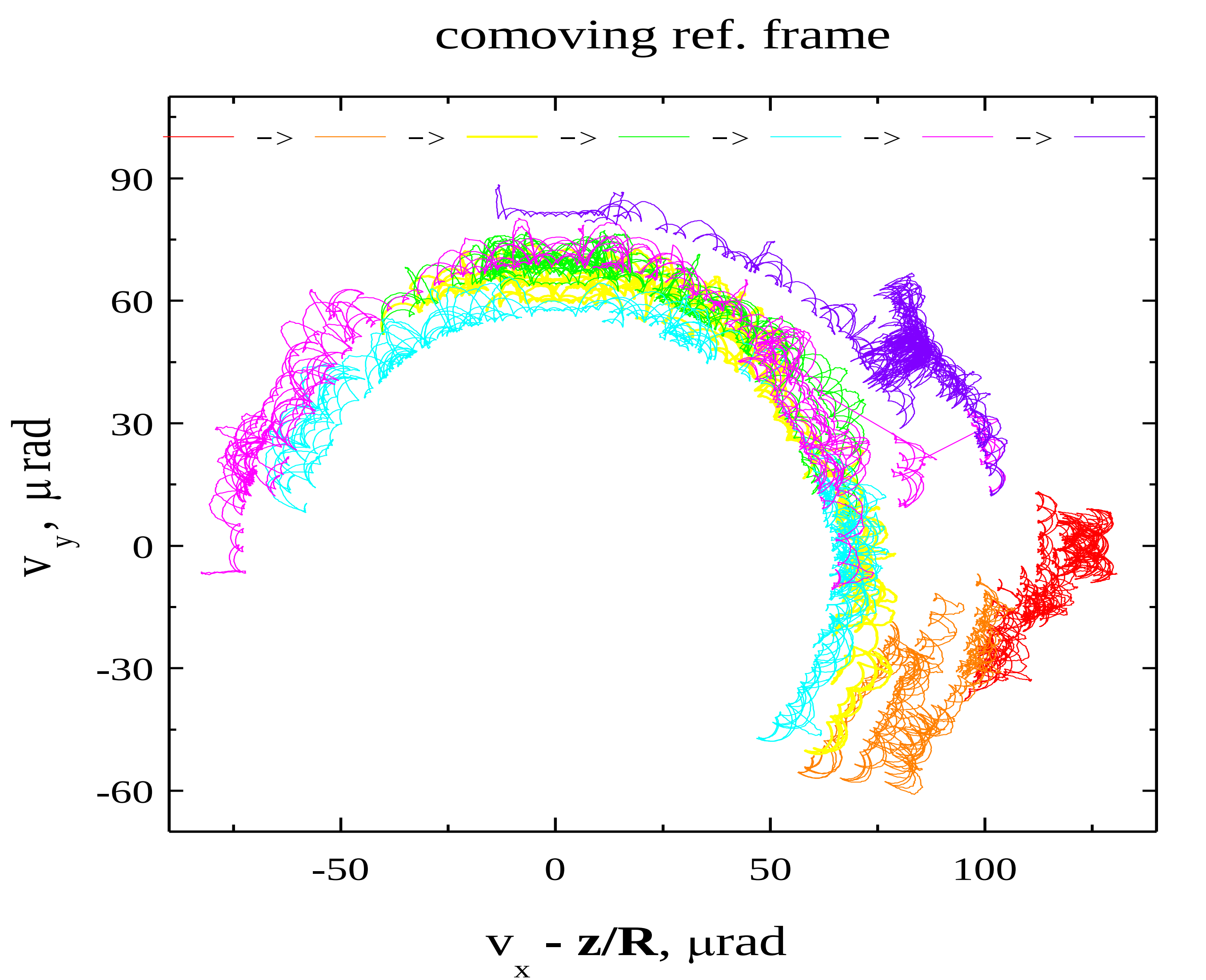

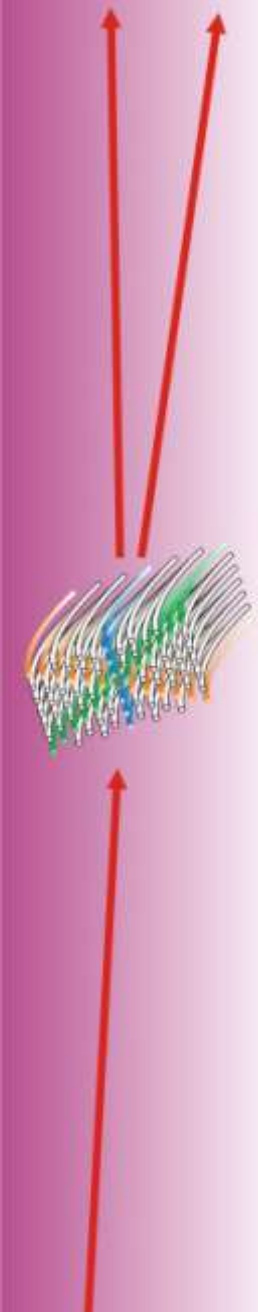

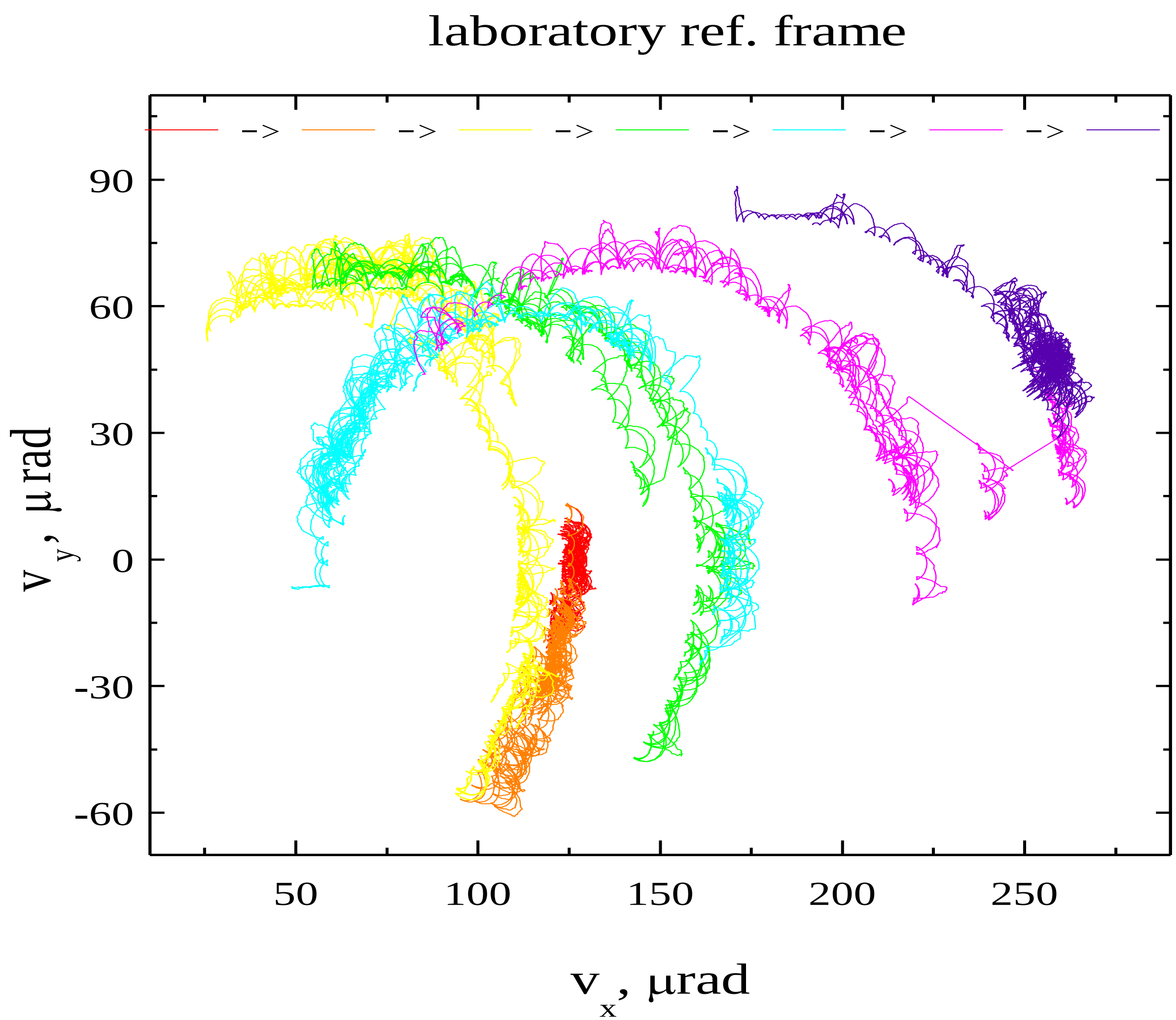

MVR manifests itself
at smallest incidence angles!

A trajectory in lab. ref. frame

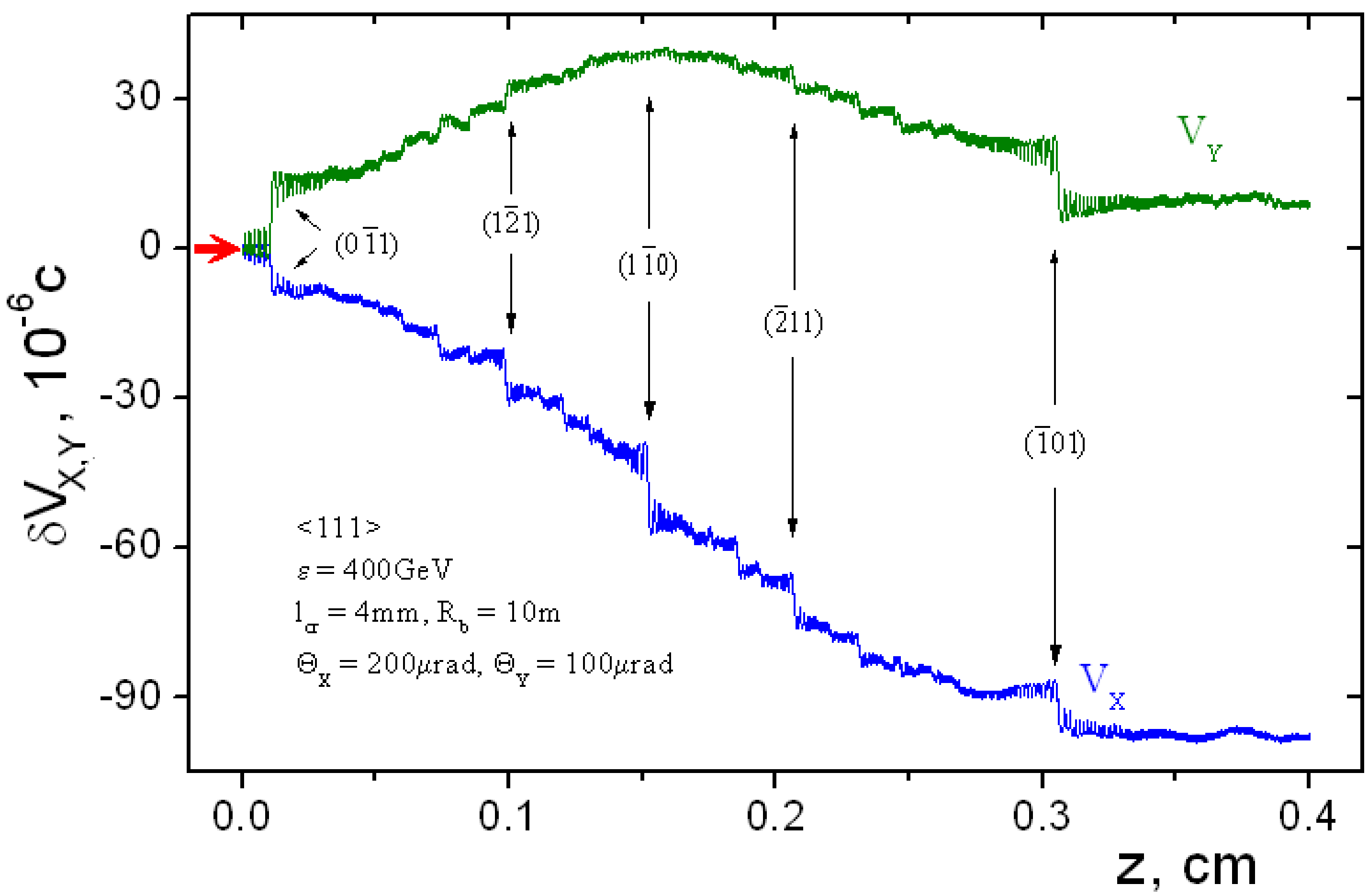

Trajectories under multiple volume reflection in comoving ref. frame

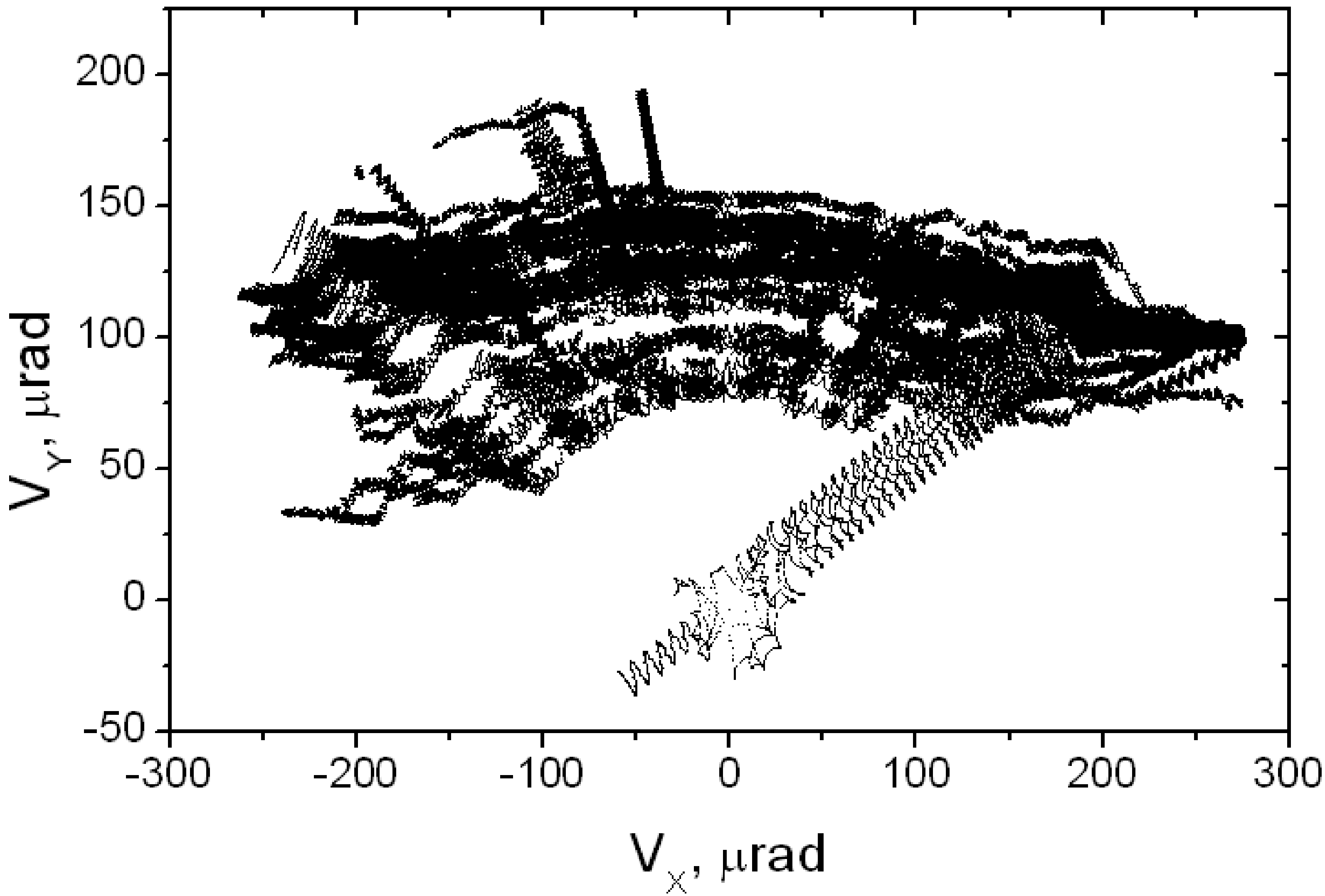

However incoherent
(one atom) scattering
remains quantum
at any energy!

Modified incoherent scattering probability (cross section times nuclei number density)

$$\frac{dP(\vec{\rho},\vec{q})}{dz}=\frac{dP(x,\vec{q})}{dz}=\frac{4Z^2\alpha^2 n_0 d_{\mathrm{pl}}}{\pi v^2}\int_{-\infty}^{\infty}\frac{\cos(\kappa x)\left\{\exp\left(-2\kappa^2 u_1^2\right)-\exp\left[-\left(q_x^2+\kappa^2\right)u_1^2\right]\right\}}{\left[\left(q_x+\kappa\right)^2+q_y^2+\kappa_s^2\right]\left[\left(q_x-\kappa\right)^2+q_y^2+\kappa_s^2\right]}d\kappa$$

Kitagava-Ohtsuki (Rutherford/Mott) limit $q_x \gg \hbar / u_1$

$$\frac{dP\left(x, q\gg 1/u_1>\kappa_s\right)}{dz}=\frac{dw_{\mathrm{loc}}(x,\vec{q})}{d^2q\,dz}=\frac{4Z^2\alpha^2}{v^2q^4}\frac{n_0 d_{\mathrm{pl}}}{\sqrt{2\pi}\,u_1}\exp\left(-\frac{x^2}{2u_1^2}\right)=\frac{4Z^2\alpha^2}{v^2q^4}n_0 d_{\mathrm{pl}}n(x)$$

“Quantum” to “classical” cross sections´ ratio

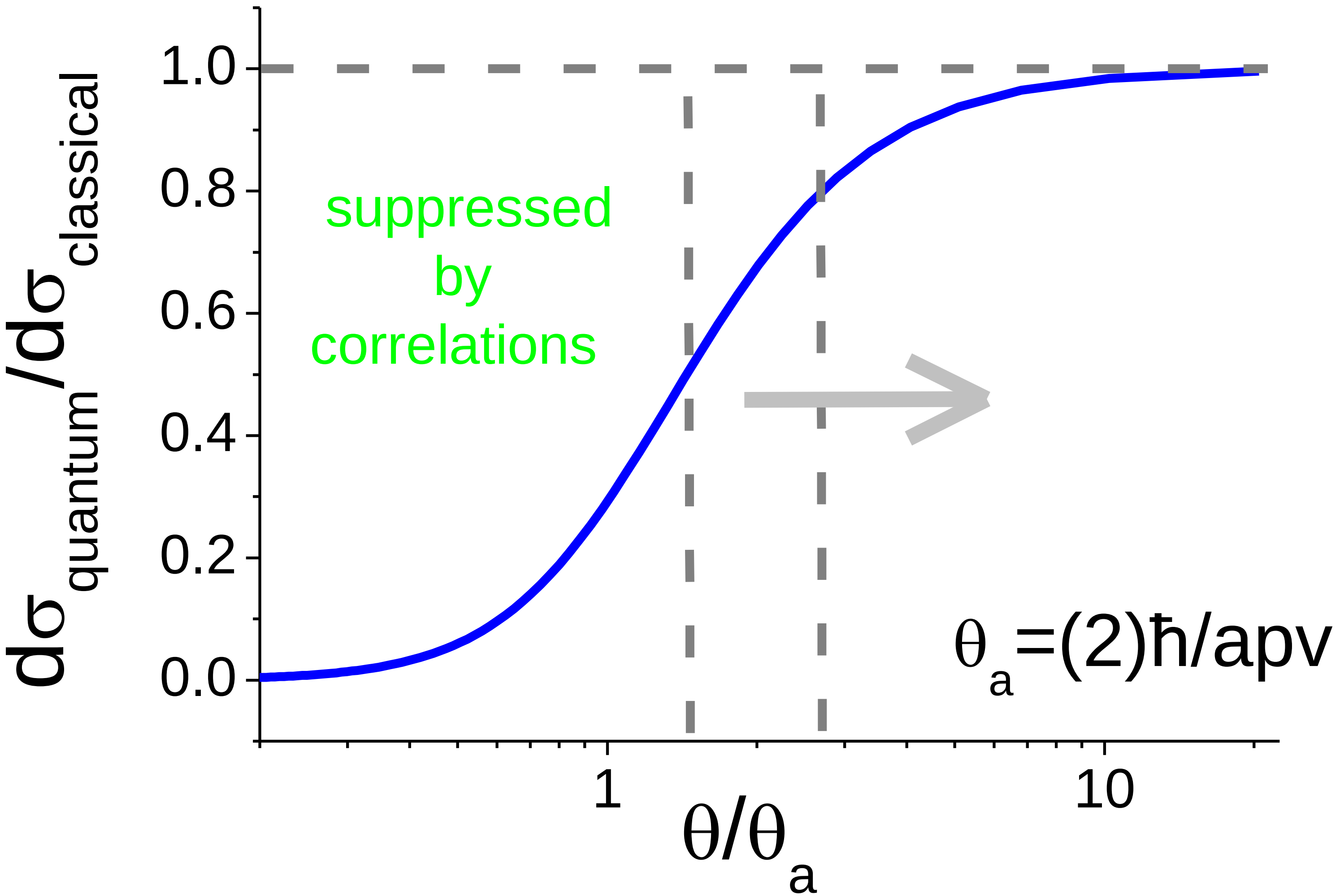

Classical mechanics overestimates scattering

Incoherent scattering probability ratio to local **Kitagava-Ohtsuki** value

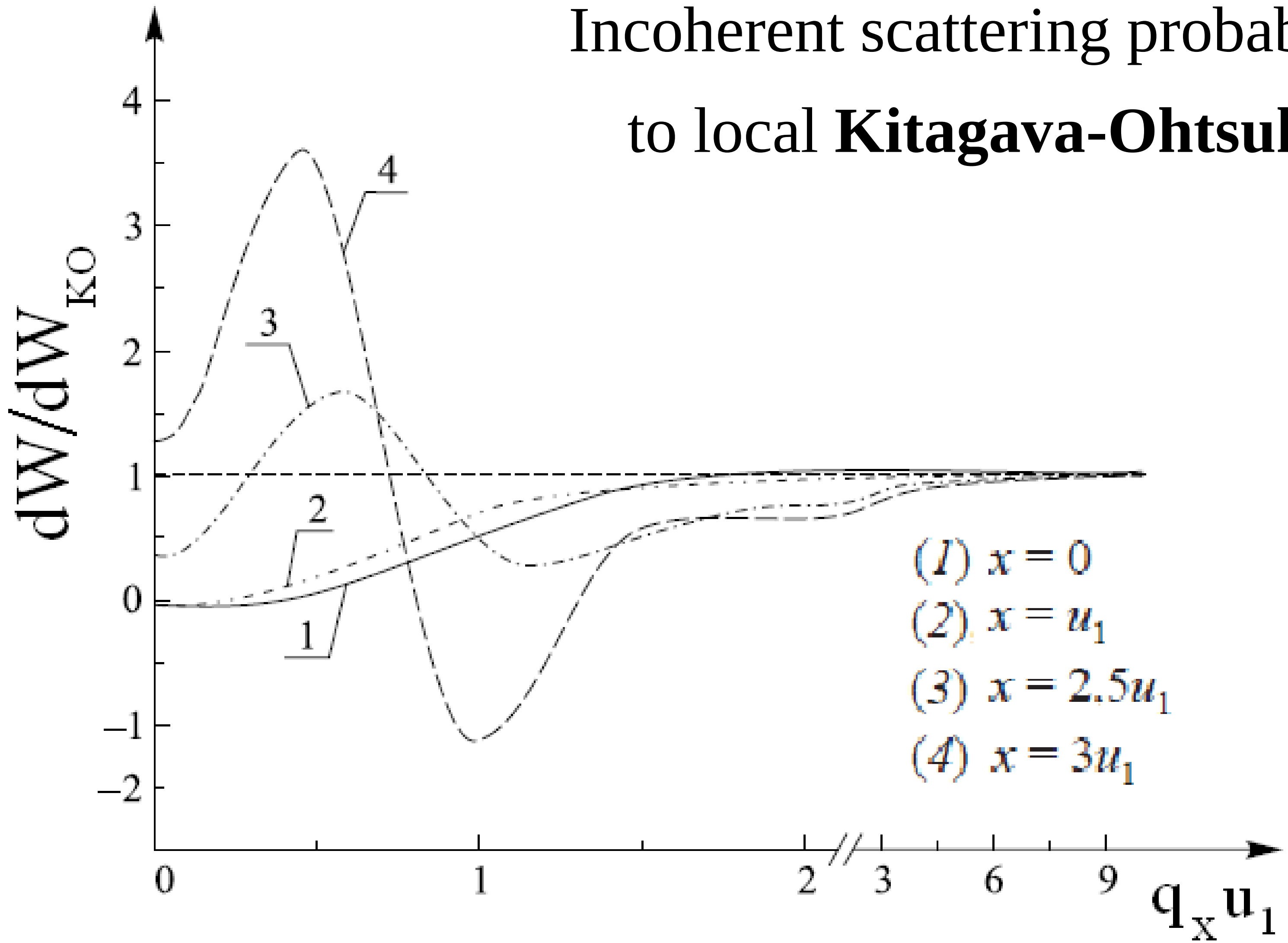

Rutherford/Mott cross section is applicable only at $q_x \gg \hbar / u_1$

Key simulation points:

Trajectory simulations in most **realistic potentials**

Simulation of **incoherent scattering** on both nuclei and electrons

Separate simulation of **single** and **multiple** scattering

Direct integration of **Baier-Katkov formula**

Infinite trajectories, **density** effect…

Radiation process simulations from the *"First Principles"*

The general expression for radiation intensity

$$\frac{d^2 I}{d\omega d^2\theta} = \frac{\alpha\omega^2 d\omega}{8\pi^2\varepsilon'^2} \times \int\int dt_1 dt_2 \left[(\varepsilon^2 + \varepsilon'^2)(\mathbf{v}_\perp(t_1) - \boldsymbol{\theta})(\mathbf{v}_\perp(t_2) - \boldsymbol{\theta}) + \omega^2/\gamma^2\right]$$

$$\exp\left\{i\frac{\omega\varepsilon}{2\varepsilon'}\left[\int_{-\infty}^{t_1}\left(\gamma^{-2} + (\mathbf{v}_\perp(t') - \boldsymbol{\theta})^2\right)dt' + \int_{-\infty}^{t_2}\left(\gamma^{-2} + (\mathbf{v}_\perp(t'') - \boldsymbol{\theta})^2\right)dt''\right]\right\}$$

contains two integrals

$$A = \int \exp\left\{i\frac{\omega\varepsilon}{2\varepsilon'}\int_{-\infty}^{t}\left[\gamma^{-2} + (\mathbf{v}_\perp(t') - \boldsymbol{\theta})^2\right]dt'\right\}dt,$$

$$\mathbf{B} = \int (\mathbf{v}_\perp(t) - \boldsymbol{\theta})\exp\left\{i\frac{\omega\varepsilon}{2\varepsilon'}\int_{-\infty}^{t}\left[\gamma^{-2} + (\mathbf{v}_\perp(t') - \boldsymbol{\theta})^2\right]dt'\right\}dt$$

and slowly decreases with radiation angle $\boldsymbol{\theta}$, complicating its numerical integration.

Radiation at sharp change of particle trajectory

$$\frac{d\mathcal{E}}{d\omega do} = \frac{e^2}{4\pi^2 c}[\boldsymbol{k}, \boldsymbol{I}]^2,$$

$$\boldsymbol{I} = \frac{ic}{\omega} \int\limits_{-\infty}^{\infty} dt\, e^{i(\omega/c)[ct - \boldsymbol{n}\cdot\boldsymbol{r}(t)]} \frac{d}{dt} \frac{\boldsymbol{v}(t)}{c - \boldsymbol{n}\cdot\boldsymbol{v}(t)}.$$

$$\boldsymbol{I} \approx \frac{ic}{\omega}\left(\frac{\boldsymbol{v}'}{c - \boldsymbol{n}\cdot\boldsymbol{v}'} - \frac{\boldsymbol{v}}{c - \boldsymbol{n}\cdot\boldsymbol{v}}\right),$$

$$\frac{d\mathcal{E}}{d\omega} = \frac{2e^2}{\pi c}\left(\frac{2\xi^2+1}{\xi\sqrt{\xi^2+1}}\ln\left(\xi + \sqrt{\xi^2+1}\right) - 1\right).$$

Single scattering effects are treated separately

$$A = \int_{-\infty}^{\infty} \exp\{i\varphi(t)\}dt = \frac{i}{\dot{\varphi}(+0)} - \frac{i}{\dot{\varphi}(-0)} +$$

$$i\sum_{i=1}^{N}\left\{\left[\frac{1}{\dot{\varphi}(t_i+0)} - \frac{1}{\dot{\varphi}(t_i-0)}\right]\exp i\varphi(t_i) - \frac{2\ddot{\varphi}(\bar{t}_i)}{\dot{\varphi}^3(\bar{t}_i)}\sin\left[\frac{\varphi(t_i-0)-\varphi(t_{i-1}+0)}{2}\right]\exp i\varphi(\bar{t}_i)\right\},$$

$$\vec{B} = \int_{-\infty}^{\infty}\left[\vec{v}_\perp(t) - \vec{\theta}\right]\exp\{i\varphi(t)\}dt = \left[\frac{i}{\dot{\varphi}(+0)} - \frac{i}{\dot{\varphi}(-0)}\right]\left(\vec{v}_\perp(0) - \vec{\theta}\right) +$$

$$i\sum_{i=1}^{N}\left\{\begin{array}{l}\left[\underline{\frac{\vec{v}_\perp(t_i)+\vec{\vartheta}_i-\vec{\theta}}{\dot{\varphi}(t_i+0)} - \frac{\vec{v}_\perp(t_i)-\vec{\theta}}{\dot{\varphi}(t_i-0)}}\right]\exp i\varphi(t_i) - \\ \frac{2}{\dot{\varphi}^2(\bar{t}_i)}\left[\dot{\vec{v}}_\perp(\bar{t}_i) - \left(\vec{v}_\perp(\bar{t}_i) - \vec{\theta}\right)\frac{\ddot{\varphi}(\bar{t}_i)}{\dot{\varphi}(\bar{t}_i)}\right]\sin\left[\frac{\varphi(t_i-0)-\varphi(t_{i-1}+0)}{2}\right]\exp i\varphi(\bar{t}_i)\end{array}\right\},$$

where $\omega' = \varepsilon/(\varepsilon-\omega)$, $\ddot{\varphi}(t) = \omega'\left(\vec{v}_\perp(t_i) - \vec{\theta}\right)\dot{\vec{v}}_\perp(t)$ and $\bar{t}_i = (t_i + t_{i-1})/2$.

Simulation of radiation accompanying multiple volume reflection

Radiation amplification under Multiple Volume Reflection in One Crystal (120 GeV e^-, 2 mm Si ⟨111⟩)

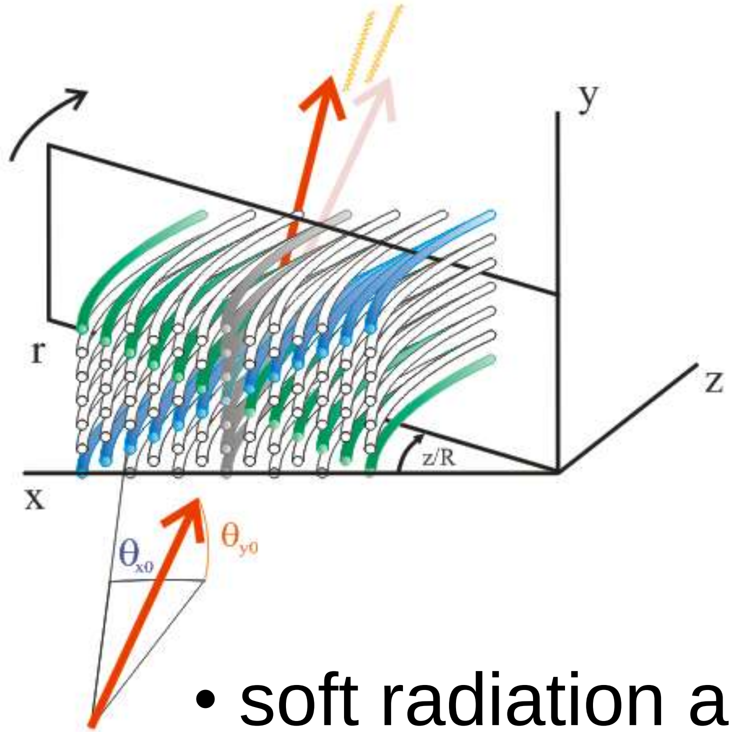

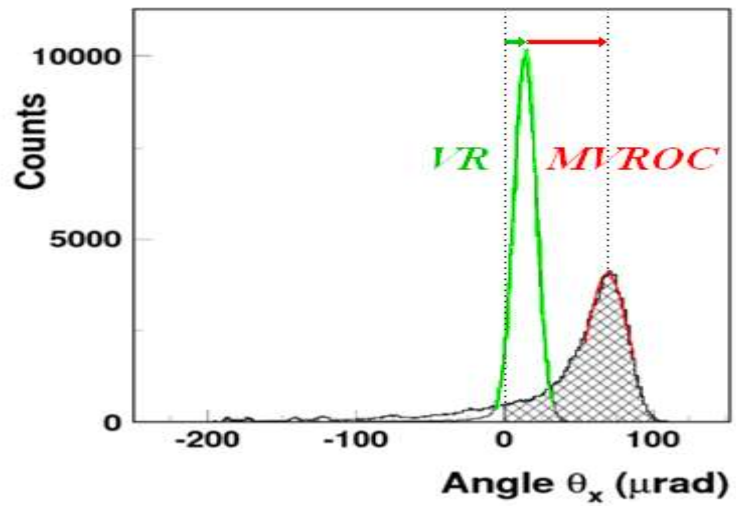

- soft radiation amplification by reflection
  by different planes
- hard radiation amplification
  by axial field

A trajectory in lab. ref. frame

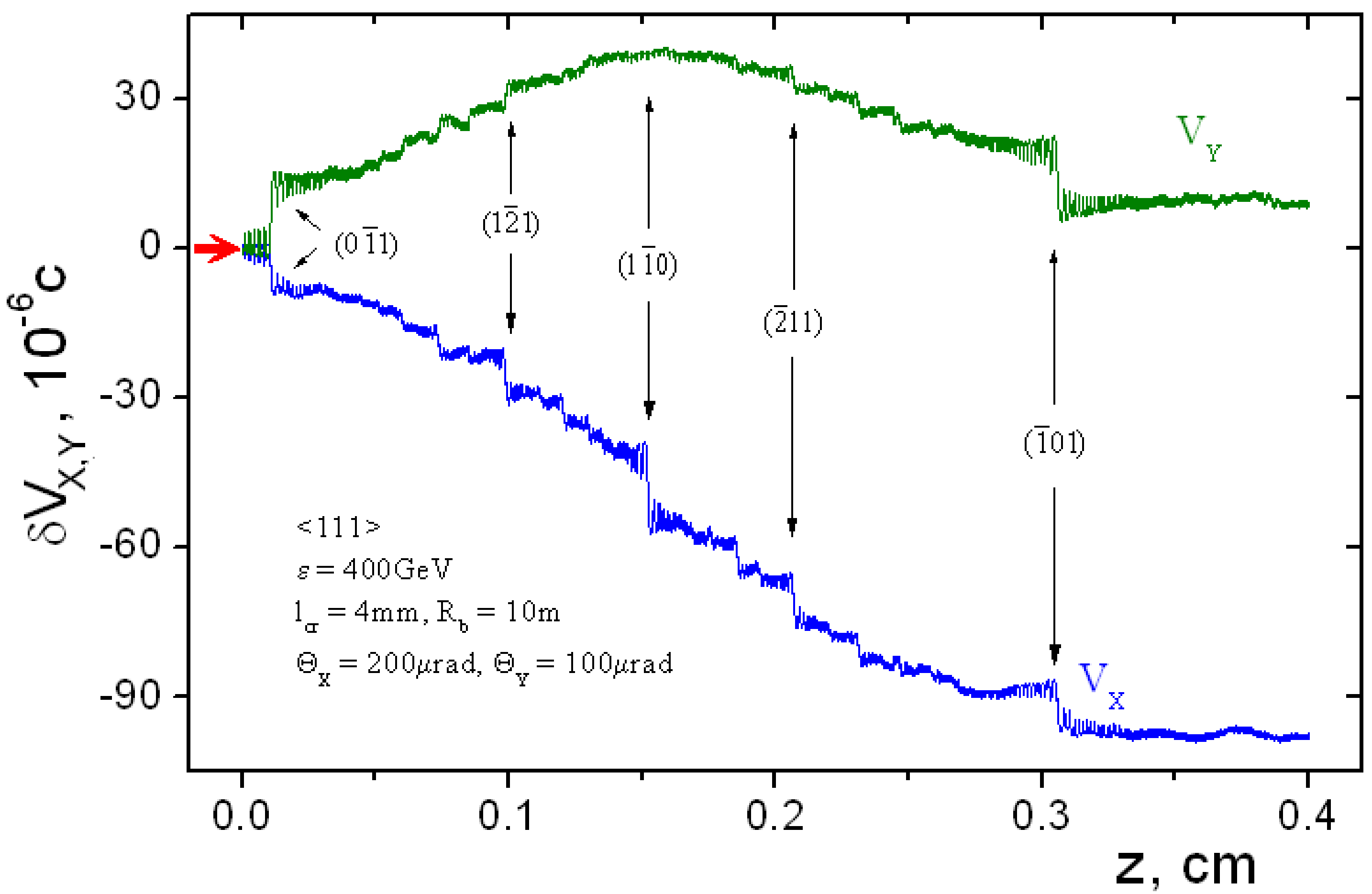

Trajectories under multiple volume reflection in comoving ref. frame

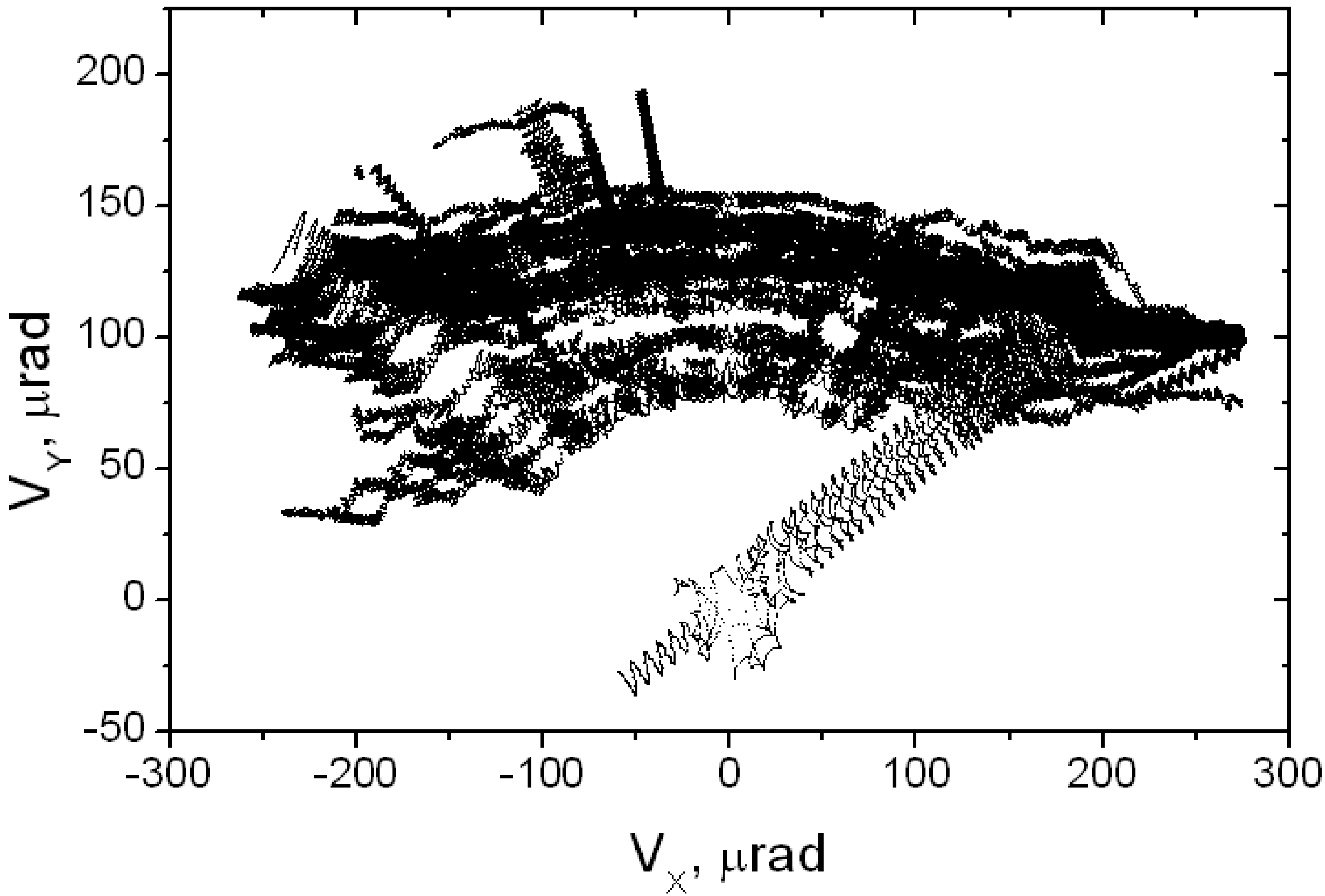

Broad and Intense Radiation Accompanying Multiple Volume Reflection of Ultrarelativistic Electrons in a Bent Crystal

L. Bandiera, E. Bagli, V. Guidi, and A. Mazzolari
INFN Sezione di Ferrara, Dipartimento di Fisica, Università di Ferrara, Via Saragat 1, 44122 Ferrara, Italy

A. Berra, D. Lietti, and M. Prest
Università dell'Insubria, Via Valleggio 11, 22100 Como, Italy, and INFN Sezione di Milano Bicocca, Piazza della Scienza 3, 20126 Milano, Italy

E. Vallazza
INFN Sezione di Trieste, Via Valerio 2, 34127 Trieste, Italy

D. De Salvador
INFN Laboratori Nazionali di Legnaro, Viale dell'Università 2, 35020 Legnaro, Italy, and Dipartimento di Fisica, Università Di Padova, Via Marzolo 8, 35131 Padova, Italy

V. Tikhomirov
Research Institute for Nuclear Problems, Belarusian State University, Minsk, Belarus
(Received 28 June 2013; published 18 December 2013)

The radiation emitted by 120 GeV/c electrons traversing a single bent crystal under multiple volume reflection orientation is investigated. Multiple volume reflection in one crystal occurs as a charged particle impacts on a bent crystal at several axial channeling angles with respect to a crystal axis. The resulting energy-loss spectrum of electrons was very intense over the full energy range up to the nominal energy of the beam. As compared to the radiation emission by an individual volume reflection, the energy-loss spectrum is more intense and peaks at an energy 3 times greater. Experimental results are compared to a theoretical approach based on the direct integration of the quasiclassical Baier and Katkov formula. In this way, it is possible to determine the mean number of photons emitted by each electron and, thus, to extract

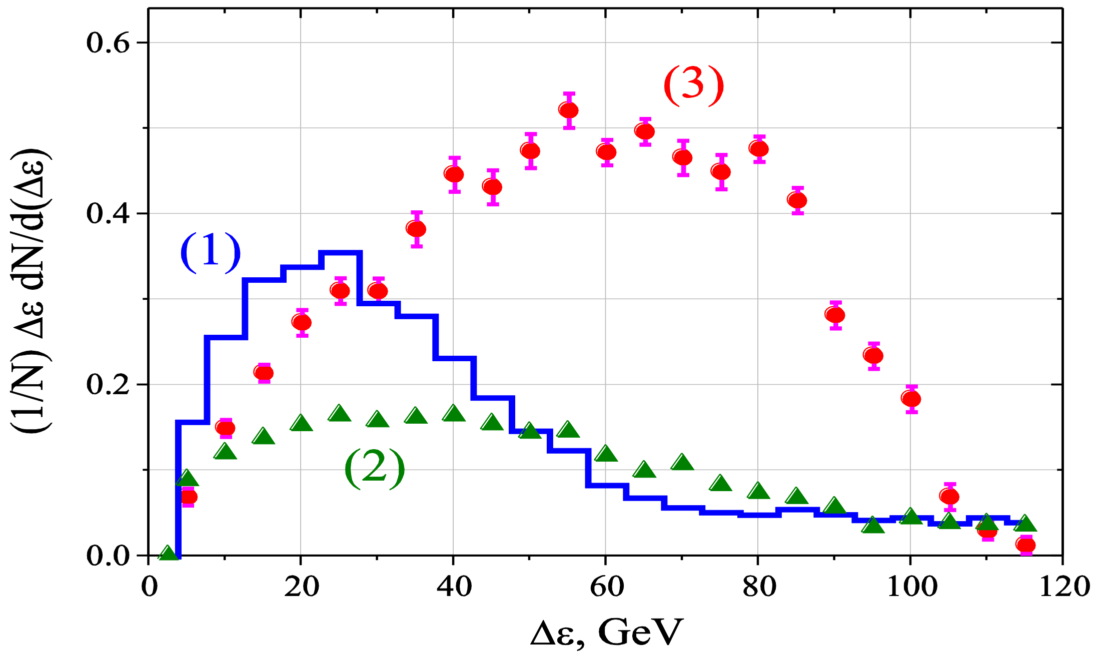

(1/N) Δε dN/d(Δε)
0.6
0.4
0.2
0.0
0
20
40
60
80
100
120
Δε, GeV
(1)
(2)
(3)

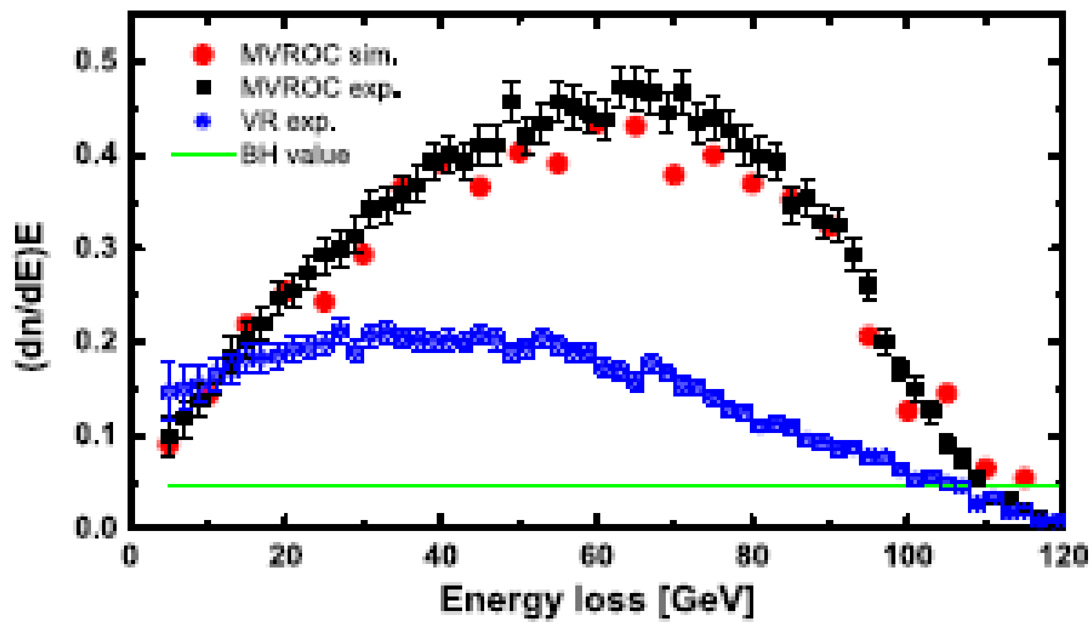

(dn/dE)E
0.5
0.4
0.3
0.2
0.1
0.0
0
20
40
60
80
100
120
Energy loss [GeV]
MVROC sim.
MVROC exp.
VR exp.
BH value

High energy electromagnetic showers in PWO

CMS ECAL is shown in green

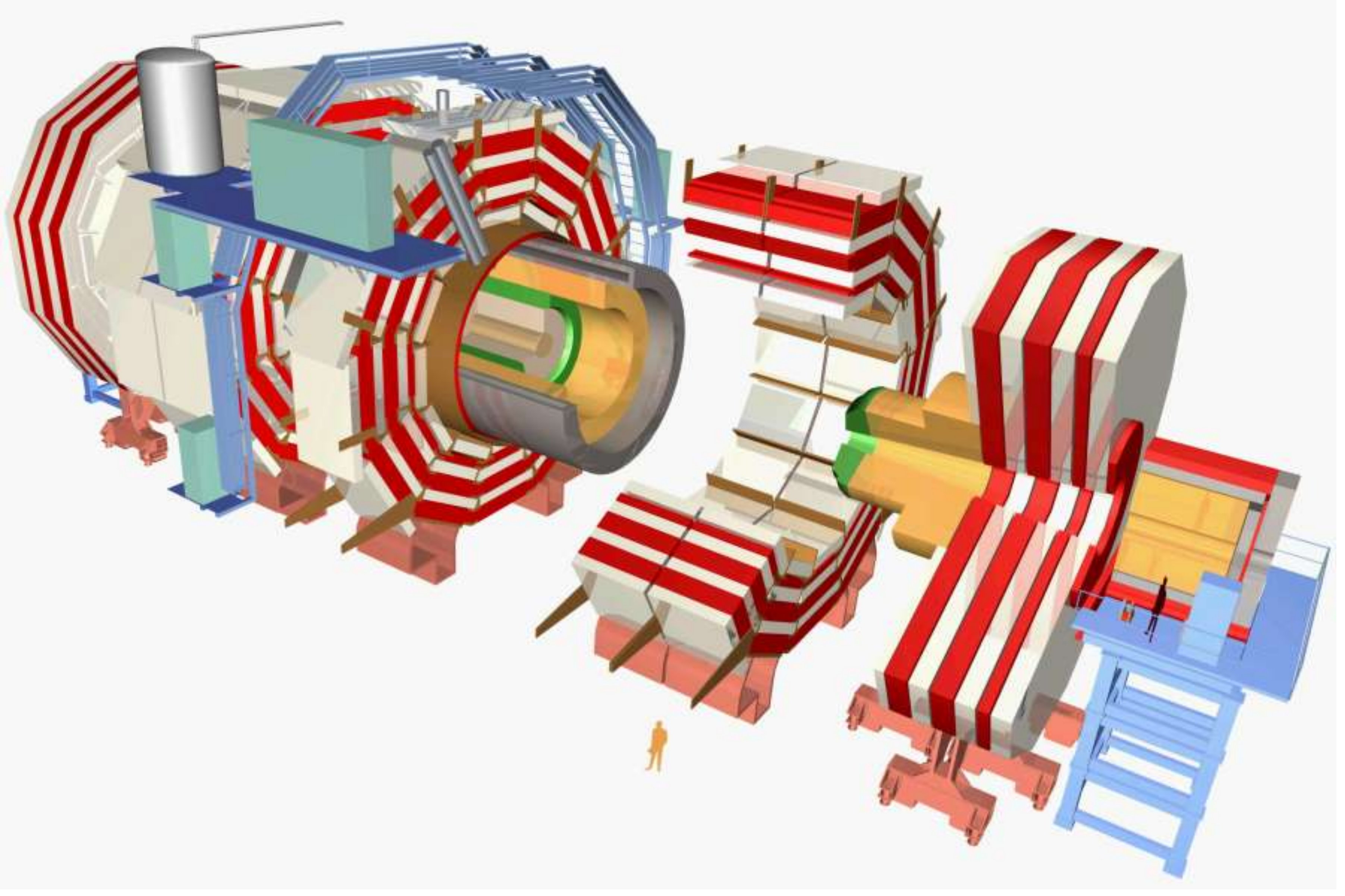

CMS

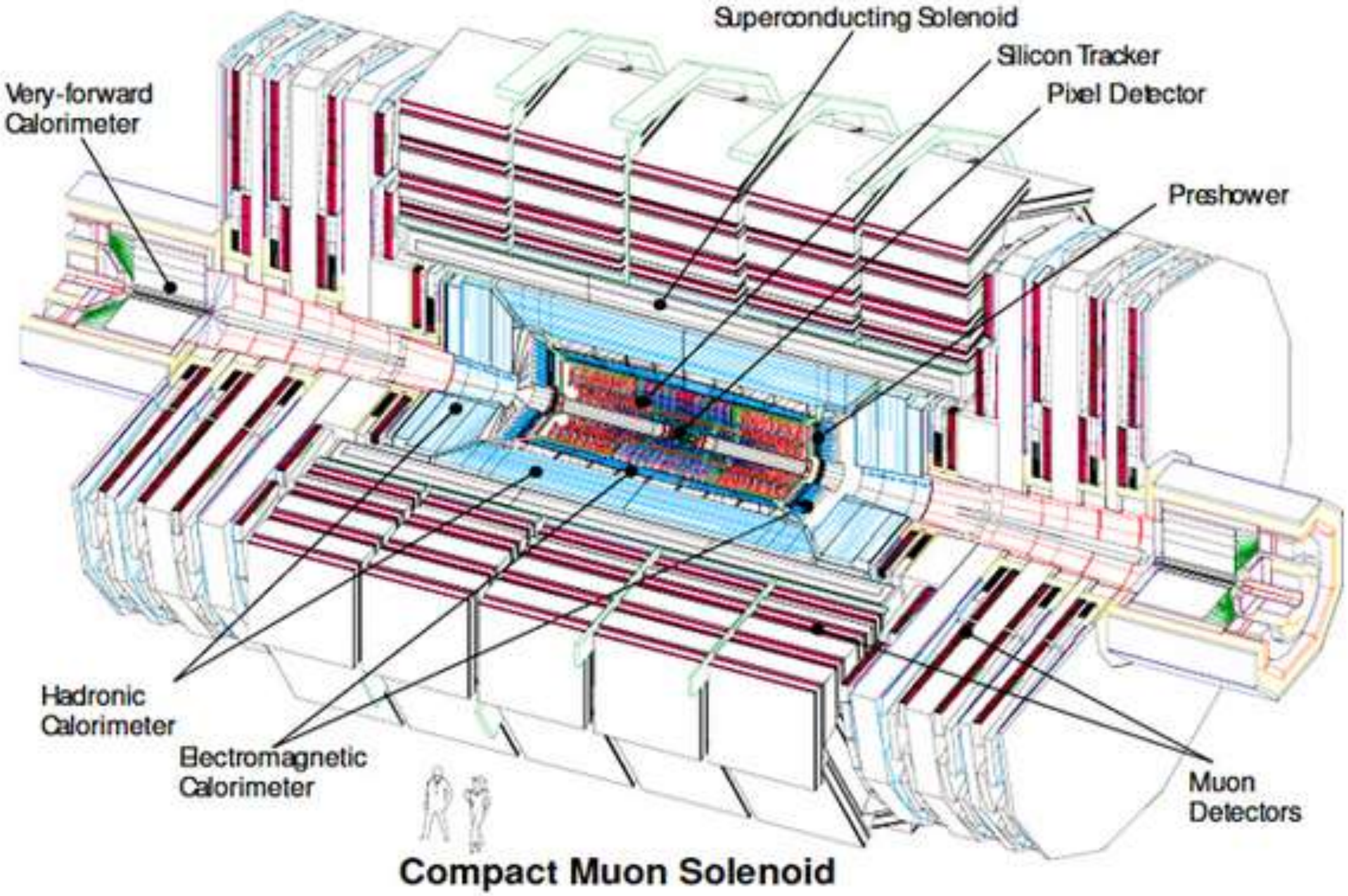
Superconducting Solenoid
Silicon Tracker
Pixel Detector
Very-forward
Calorimeter
Preshower
Hadronic
Calorimeter
Electromagnetic
Calorimeter
Muon
Detectors
Compact Muon Solenoid

CMS ECAL is made of PWO crystals

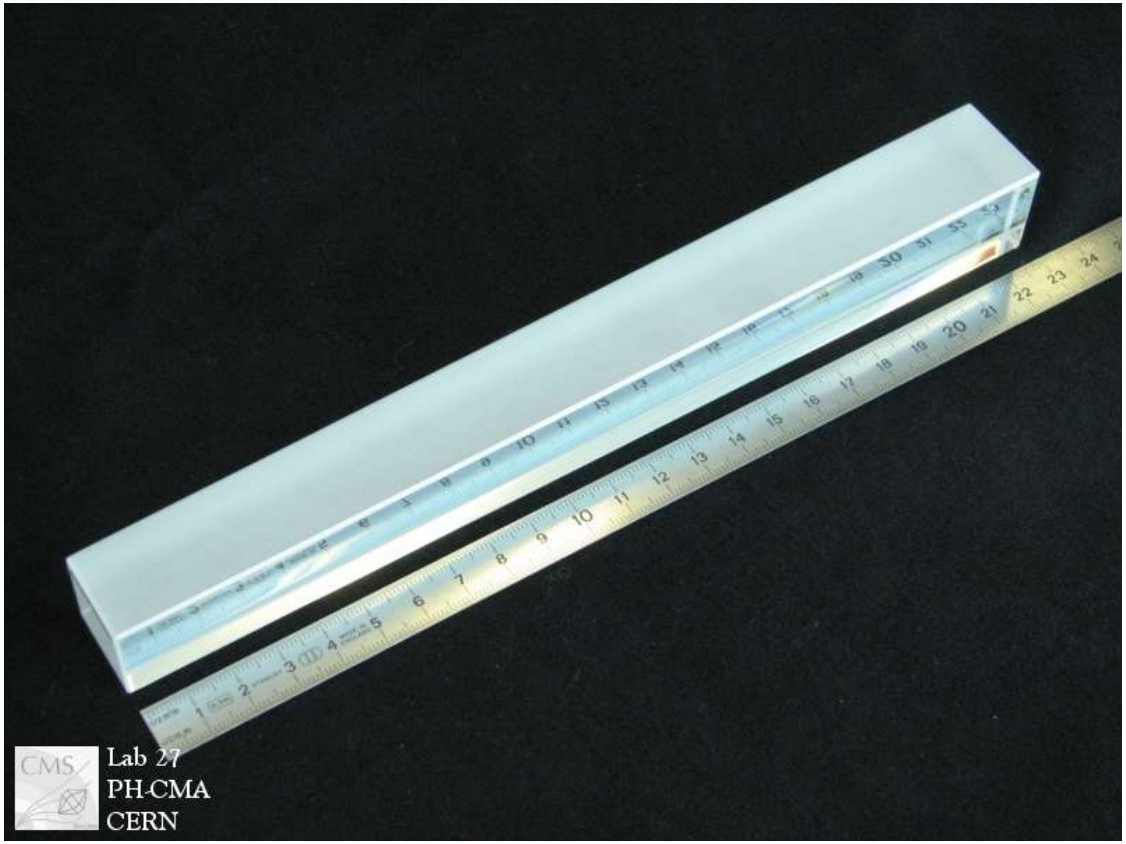

CMS TN/96-04

(19 FEB 1996)

CMS LEAD TUNGSTATE ECAL: TEST BEAM RESULTS 1995

REPORT TO THE CMS REFEREES

CMS ECAL GROUP

ABSTRACT

In the test beam in 1995 we achieved the milestone performance of an energy resolution of better than 0.6% at 100 GeV. We have demonstrated that a lead tungstate electromagnetic calorimeter read out by avalanche photodiodes can consistently achieve the excellent energy resolutions necessary to justify its construction in the CMS detector. The performance achieved, and the small differences in performance when the beam is incident on different crystals, have been understood in terms of the properties of the crystals and APDs.

..small **differences in performance** when the beam is incident on **different crystals**, have been understood in terms of the properties of the crystals and APDs.

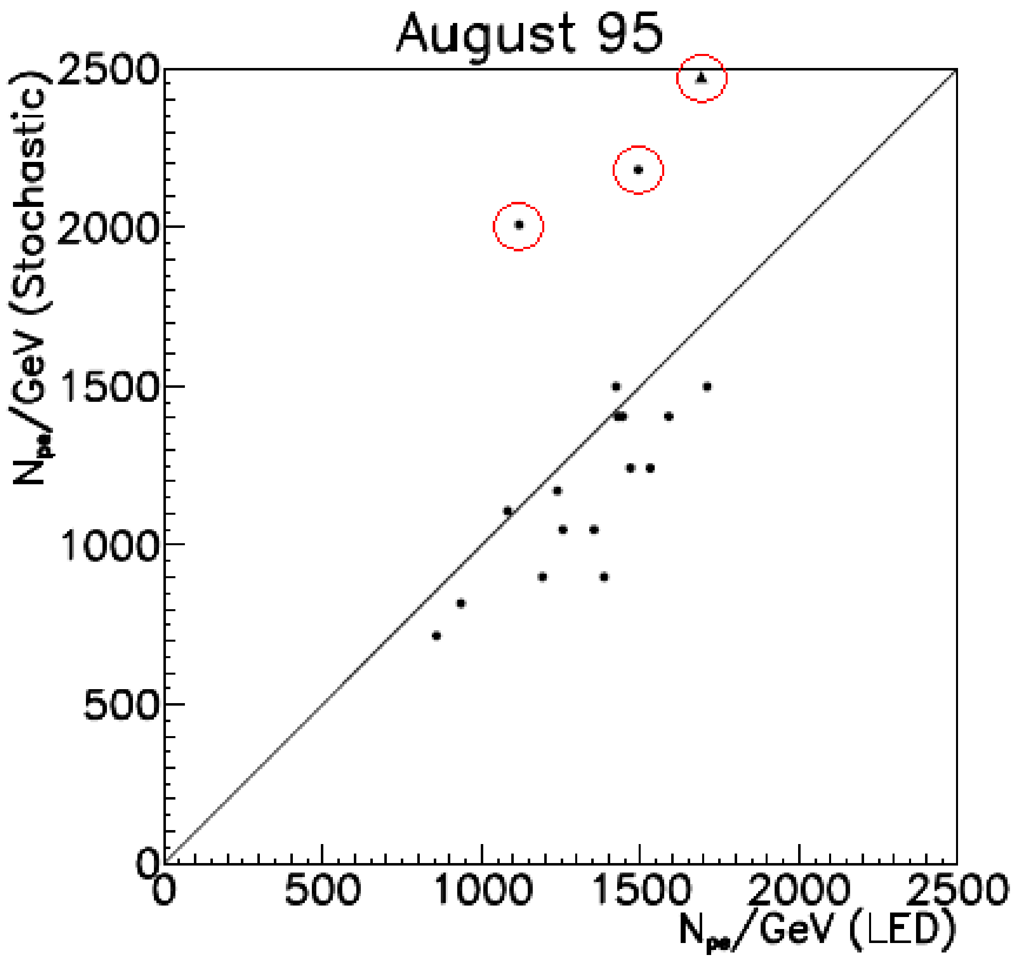

Figure 9: Photoelectron yield in 18 APDs of the August matrix as calculated from LED signals compared to photoelectron yield as calculated from the stochastic term of the measured energy resolution function

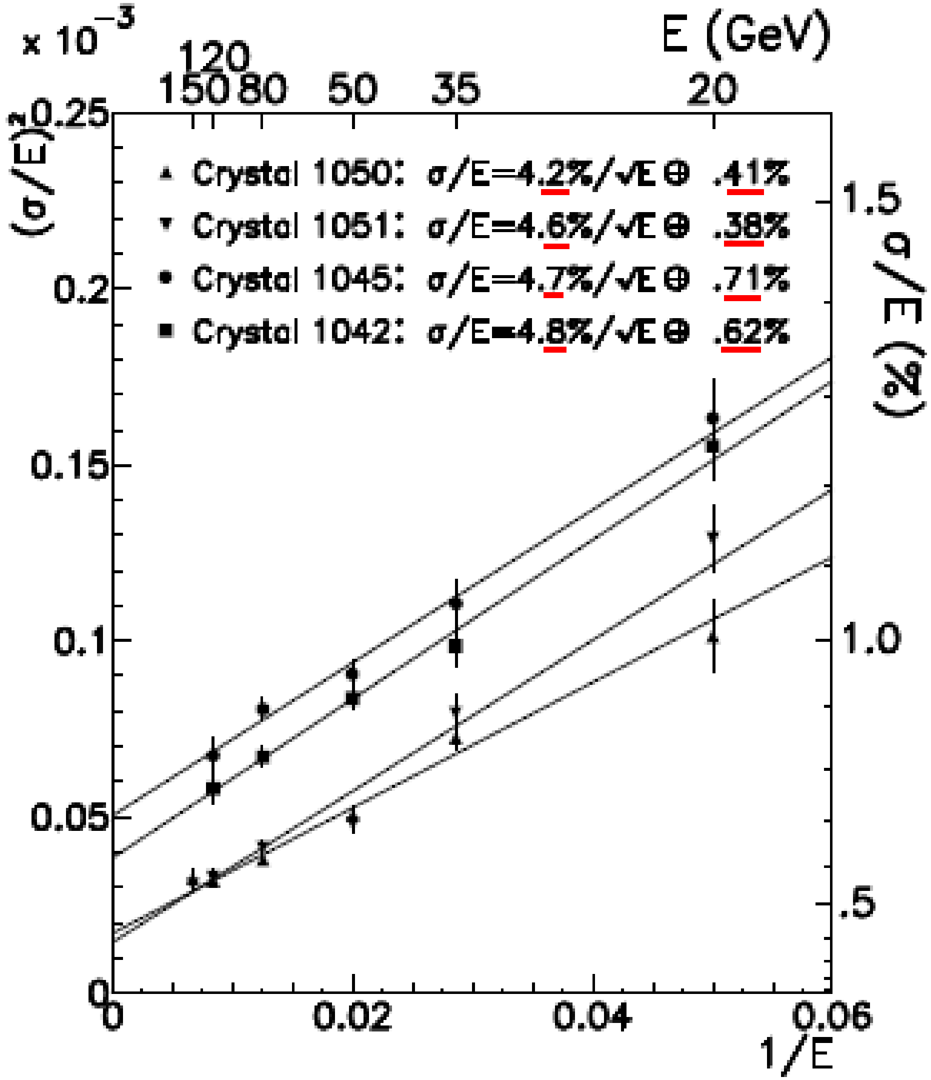

Figure 11: Energy resolution (after noise subtraction) as a function of energy for the 4 central towers

Available on CMS information server

CMS NOTE 1998/031

The Compact Muon Solenoid Experiment

CMS Note

Mailing address: CMS CERN, CH-1211 GENEVA 23, Switzerland

12 January 1998

Comparison of electromagnetic shower profile in 1996 test beam and GEANT simulation

K. Lassila-Perini

Institute of Particle Physics (IPP), ETHZ, CH-8093 Zürich, Switzerland

Abstract

the GEANT simulation has a tendency to **overestimate the shower dimensions**. A very good agreement is obtained if the lateral width of the GEANT shower is reduced by 6%.

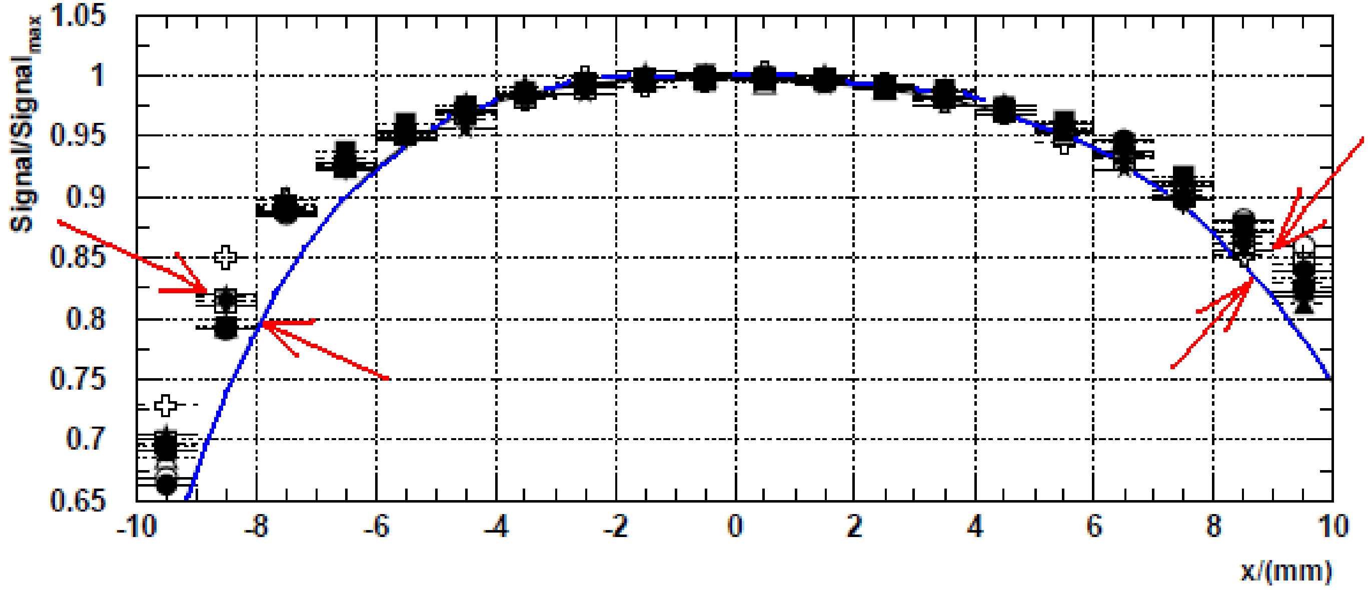

The energy containment as a function of the impact point.

Only too large increase of the lateral crystal dimensions and variations of both the width of the gap between the crystals and the tilt angle can explain the observed discrepancy

Discussing PWO problems in Minsk 1999

*J*inst

PUBLISHED BY IOP PUBLISHING FOR SISSA MEDIALAB

RECEIVED: *June 9, 2013*
ACCEPTED: *August 8, 2013*
PUBLISHED: *September 19, 2013*

Energy calibration and resolution of the CMS electromagnetic calorimeter in pp collisions at $\sqrt{s} = 7$ TeV

The CMS collaboration

E-mail: cms-publication-committee-chair@cern.ch

The resolution in simulation is better than in data.

For both the electrons from Z-boson decays and the photons from Z $\rightarrow$ μμγ, the **energy resolution** in the data is **not correctly described by the MC simulation**.

The sources of this Discrepancy are thought to be **common**.

These differences are accommodated in CMS analyses by applying **additional Gaussian smearing**.

Joint FIAL−MIPHY−Protvino PWO effort, 1999

ELSEVIER

3 June 1999

PHYSICS LETTERS B

Physics Letters B 456 (1999) 86–89

Electromagnetic cascades in oriented crystals of garnet and tungstate

V.A. Baskov [a], A.P. Bugorsky [b], V.A. Kachanov [b], V.A. Khablo [a], V.V. Kim [a], B.I. Luchkov [c], A.P. Meschanin [b], A.I. Mysnik [b], V.V. Poliansky [a], V.I. Sergienko [a,1], V.Yu. Tugaenko [c], A.N. Vasil'ev [b]

[a] *P.N.Lebedev Physical Institute, 117924 Moscow, Russian Federation*
[b] *High Energy Physics Institute, 142284 Protvino, Russian Federation*
[c] *Physical Engineering Institute, 115409 Moscow, Russian Federation*

We present experimental data on characteristics of peculiar electromagnetic cascades initiated by **26 GeV** electrons in transparent oriented crystals of artificial garnet and **lead tungstate**.

An enhancement of the mean energy deposition was observed

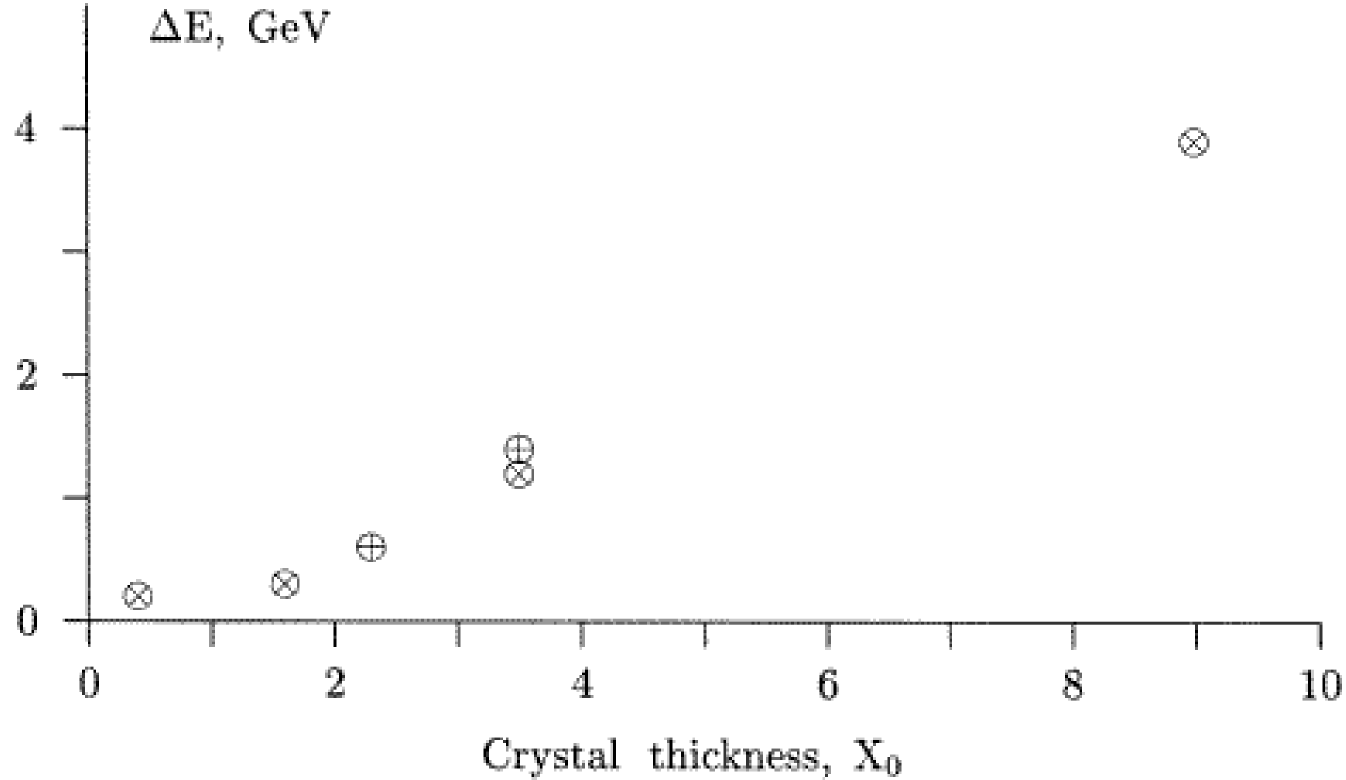

Fig. 1. The enhancement of the mean energy deposition in the garnet (⊗) and the lead tungstate (⊕) crystals.

At LHC energies the cascade can cross several radiators. If the direction of the crystallographic axis in some of the radiators is close to the direction of the cascade, more energy will be deposited in that radiator. As a result of the Redistribution of the energy depositions in the radiator cells, the reconstruction of **the primary γ-quantum impact point will be done with deteriorated accuracy**.

such results are necessary for developing a reliable Monte Carlo code for simulating peculiar cascades in compound crystals and for the design of calorimeters with oriented short crystalline radiators.

discussed... the possibility of constructing a γ-telescope of **high angular resolution** which would be able to resolve point-like sources of g-quanta of energies above 1 GeV.

Strong Reduction of the Effective Radiation Length in an Axially Oriented Scintillator Crystal

L. Bandiera,[1,*] V. V. Tikhomirov,[2] M. Romagnoni,[1] N. Argiolas,[3] E. Bagli,[1] G. Ballerini,[4] A. Berra,[4] C. Brizzolari,[4] R. Camattari,[1] D. De Salvador,[3] V. Haurylavets,[2] V. Mascagna,[4] A. Mazzolari,[1] M. Prest,[4] M. Soldani,[4] A. Sytov,[1,2] and E. Vallazza[5]
[1]*INFN Sezione di Ferrara and Dipartimento di Fisica e Scienze della Terra, Università degli Studi di Ferrara Via Saragat 1, 44122 Ferrara, Italy*
[2]*Institute for Nuclear Problems, Belarusian State University, 220030 Minsk, Belarus*
[3]*INFN Sezione di Legnaro and Dipartimento di Fisica e Astronomia, Università degli Studi di Padova, 35131 Padova, Italy*
[4]*INFN Sezione di Milano Bicocca and Dipartimento di Scienza e Alta Tecnologia, Università degli Studi dell'Insubria Via Valleggio, 22100 Como, Italy*
[5]*INFN Sezione di Trieste, Via Valerio 2, 34149 Trieste, Italy*

(Received 2 May 2018; published 12 July 2018)

We measured a considerable increase of the emitted radiation by 120 GeV/c electrons in an axially oriented lead tungstate scintillator crystal, if compared to the case in which the sample was not aligned with the beam direction. This enhancement resulted from the interaction of particles with the strong crystalline electromagnetic field. The data collected at the external lines of the CERN Super Proton Synchrotron were critically compared to Monte Carlo simulations based on the Baier-Katkov quasiclassical method, highlighting a reduction of the scintillator radiation length by a factor of 5 in the case of beam alignment with the [001] crystal axes. The observed effect opens the way to the realization of compact electromagnetic calorimeters or detectors based on oriented scintillator crystals in which the amount of material can be strongly reduced with respect to the state of the art. These devices could have relevant applications in fixed-target experiments, as well as in satellite-borne γ telescopes.

DOI: 10.1103/PhysRevLett.121.021603

Dr. Laura Bandiera

120 GeV electron radiation in <001> PWO

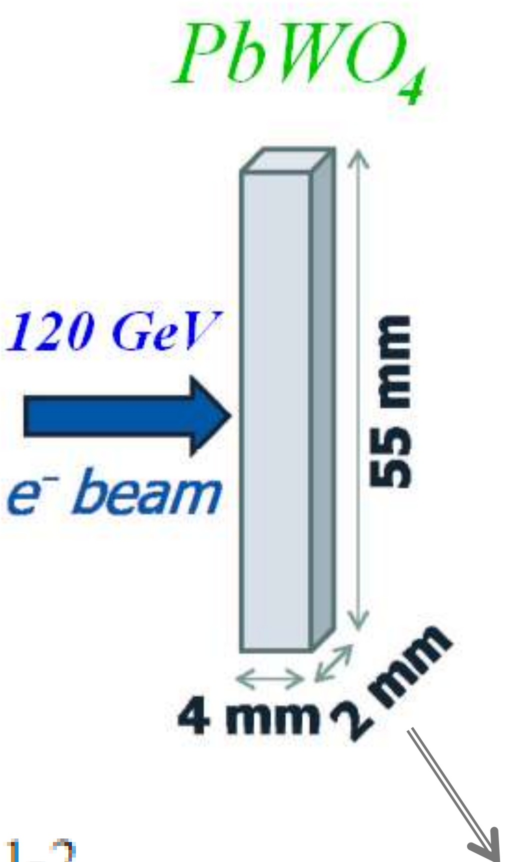

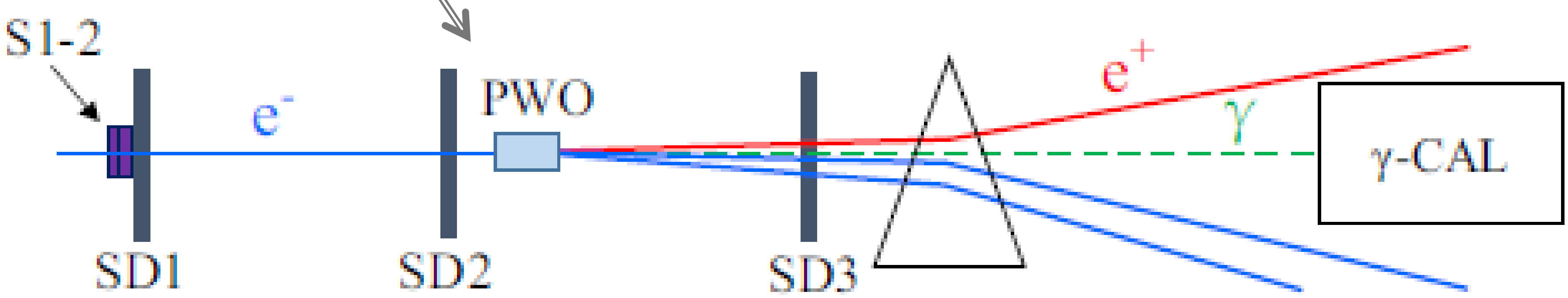

120 GeV electron radiation in <001> PWO

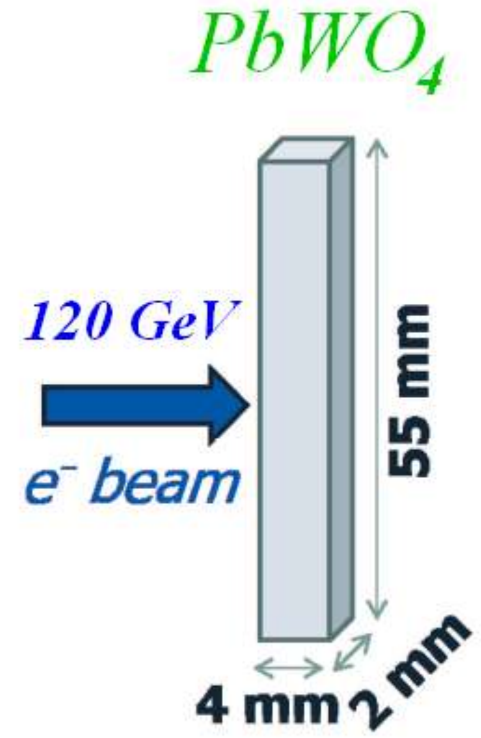

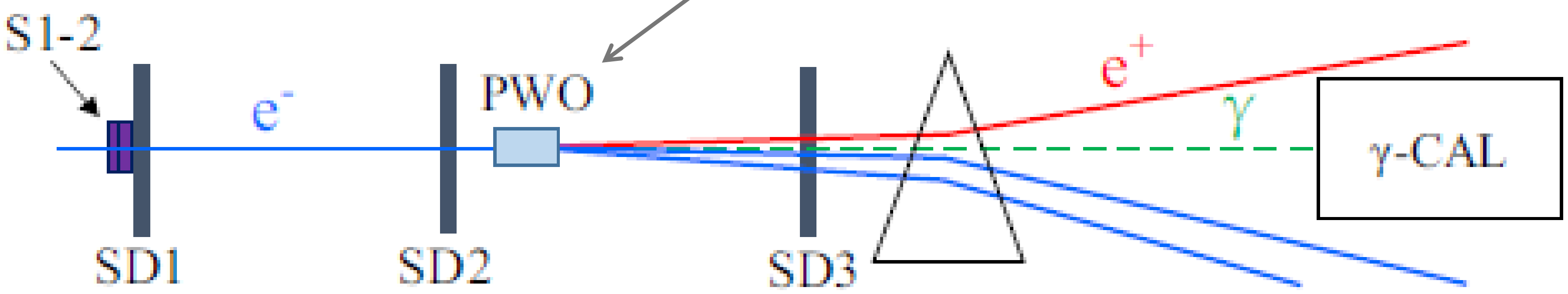

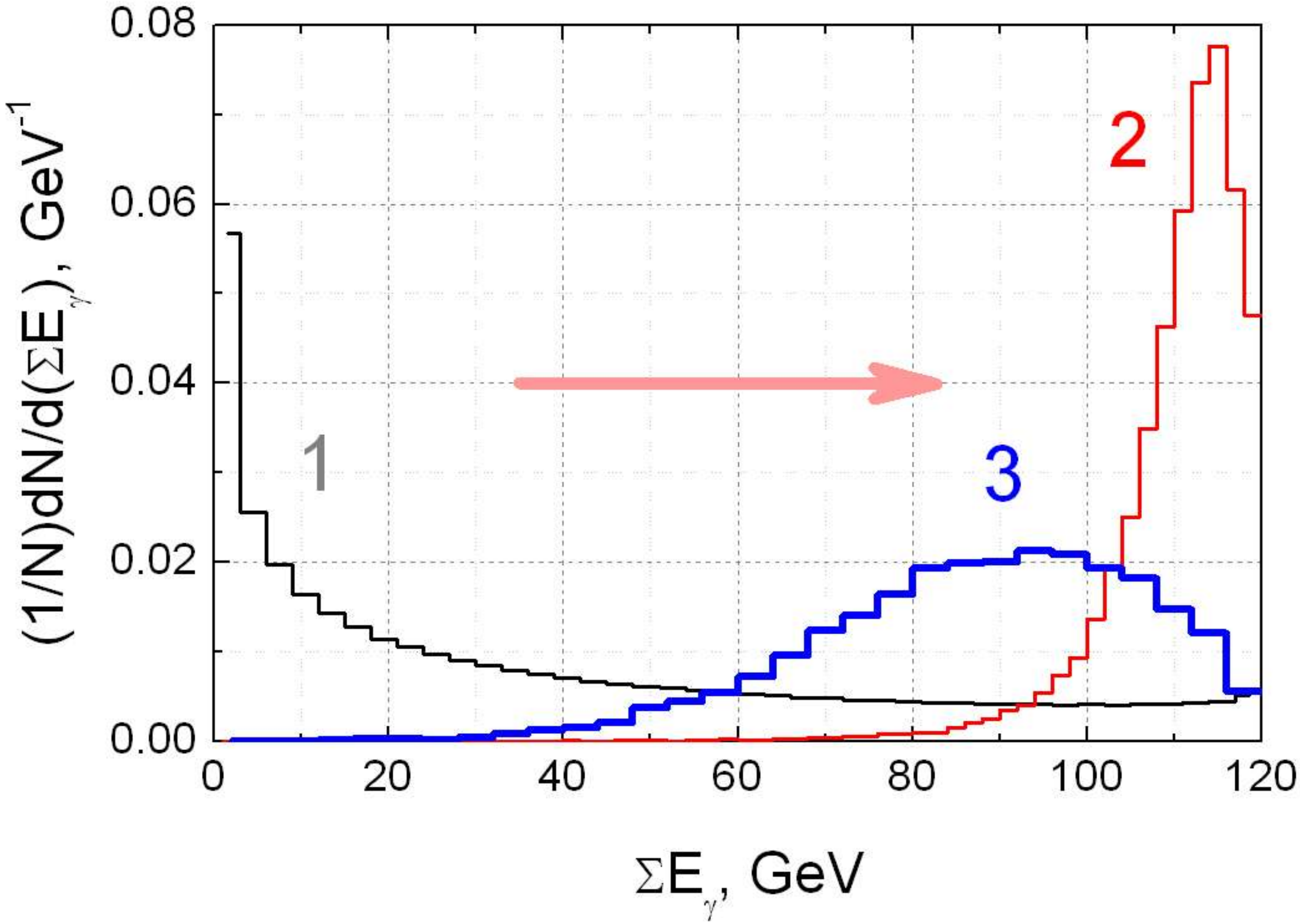

120 GeV electron energy losses on 4 mm of **amorphous** $PbWO_4$ (1), crystalline $PbWO_4$ with (**3**) and **without** (**2**) PP by radiated photons

Electromagnetic shower development acceleration in PWO at E_e =120 GeV

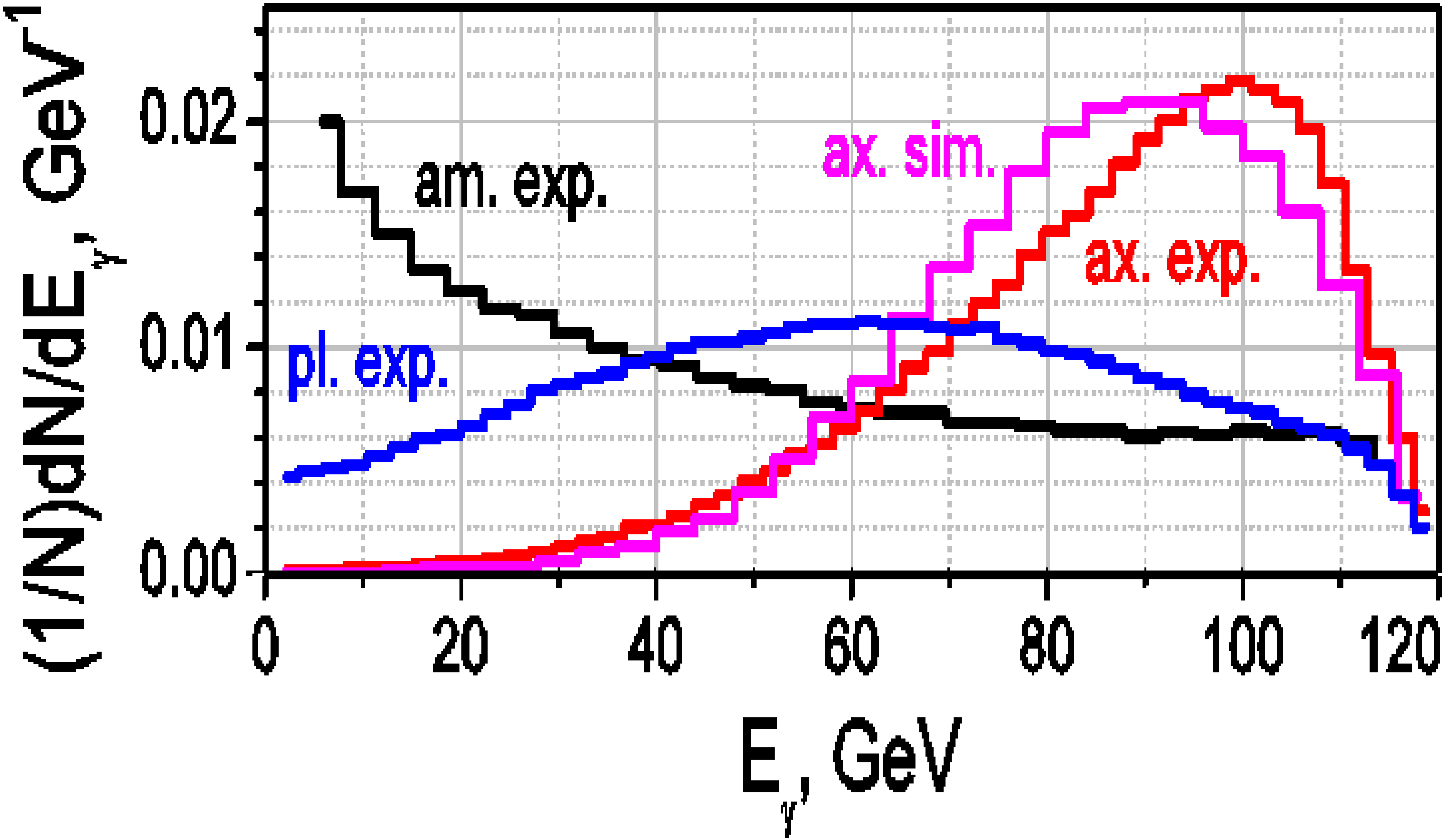

First simulations of shower development in ECAL CMS

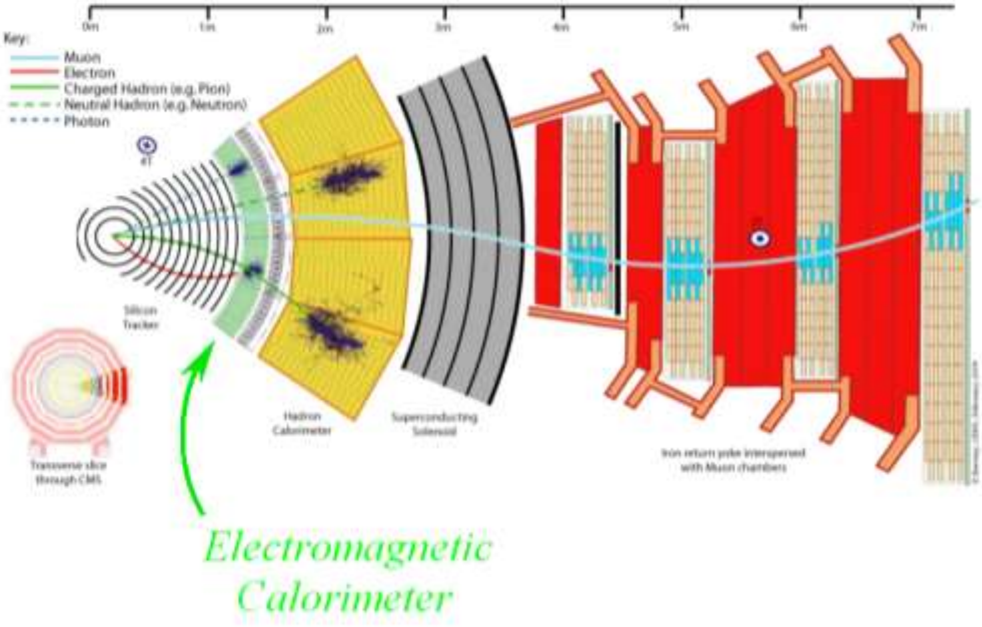

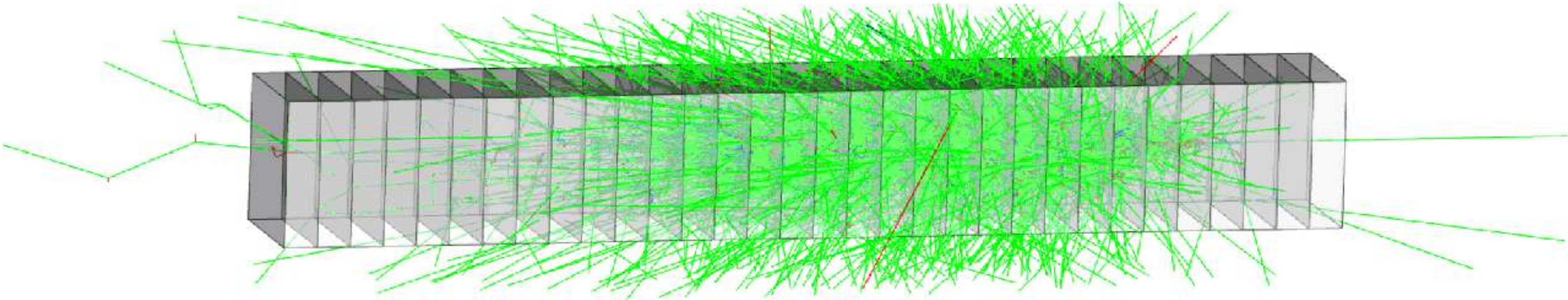

ЭМ-ливень в камере Вильсона со свинцовыми пластинами

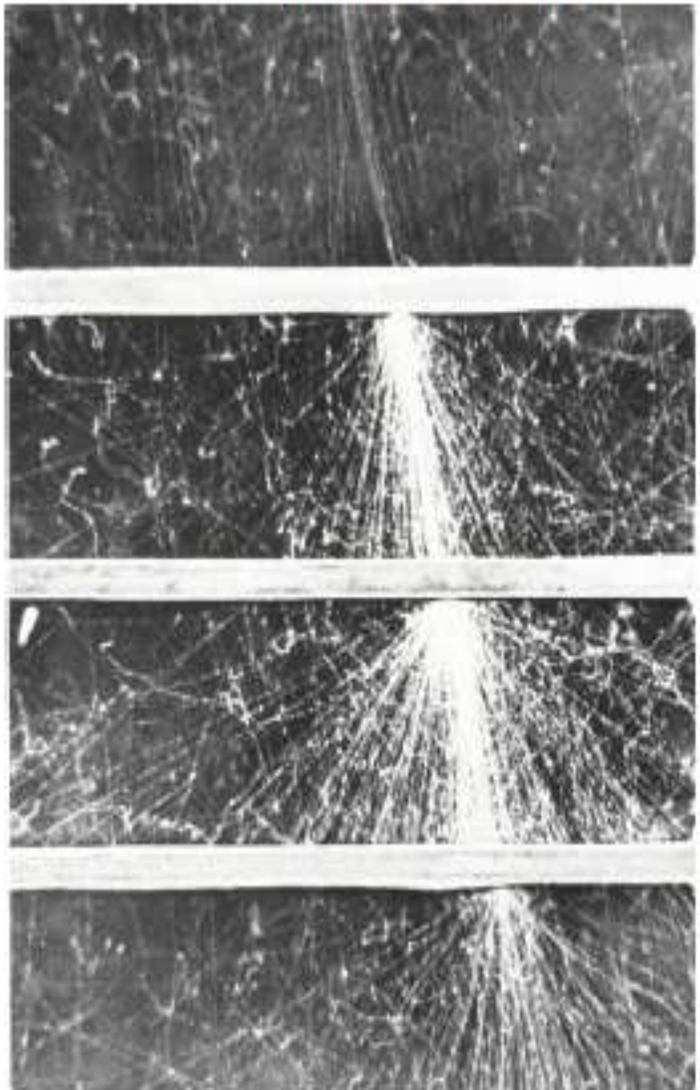

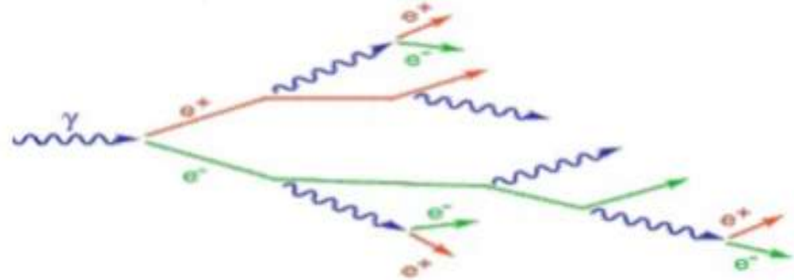

Схема электромагнитного ливня.

Run 308 Event 332 Collection view

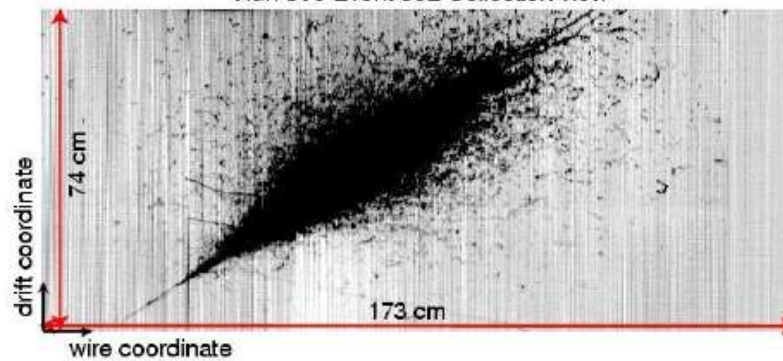

Electromagnetic shower observed in the ICARUS LAr drift chamber during the technical run with cosmic rays at Pavia, summer 2001

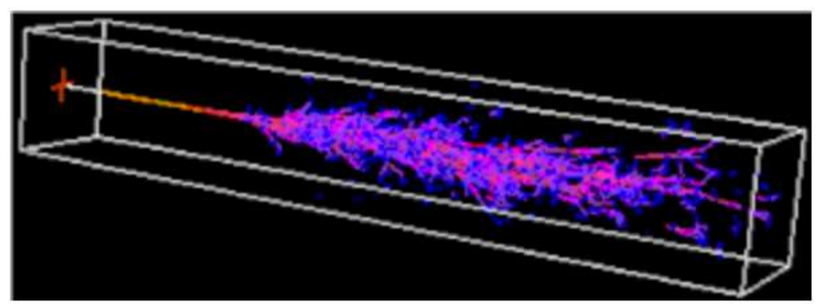

Монте-Карло симулирование электронного ливня в кристалле.

Electromagnetic shower acceleration in PWO at 50, 100 and 1000 GeV

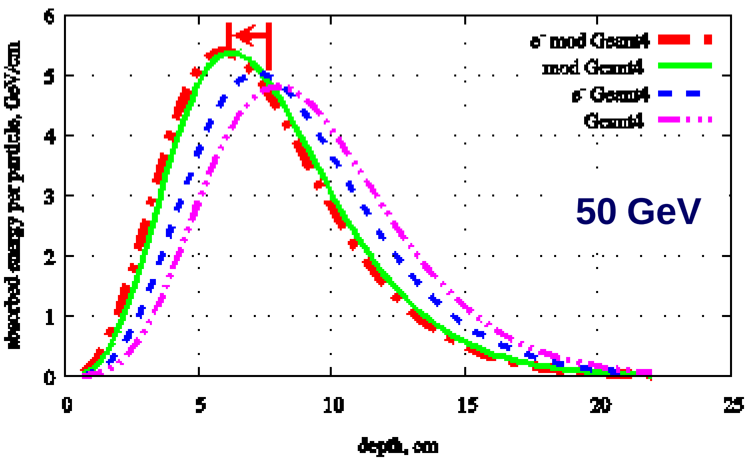

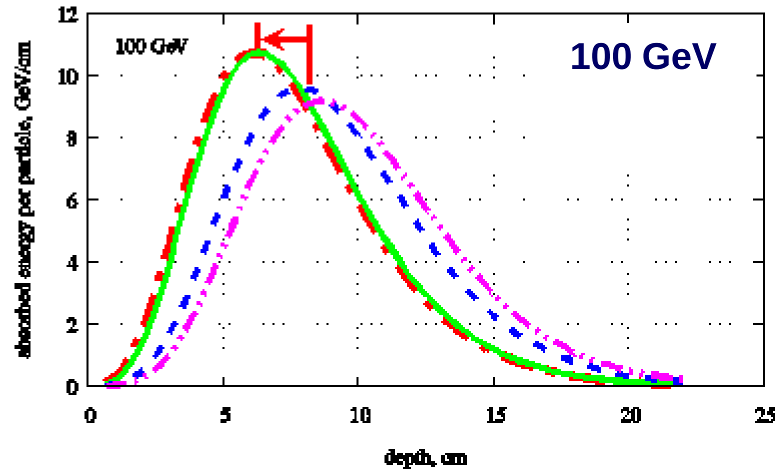

em shower maximum shifts

by 2 ÷ 5

radiation lengths

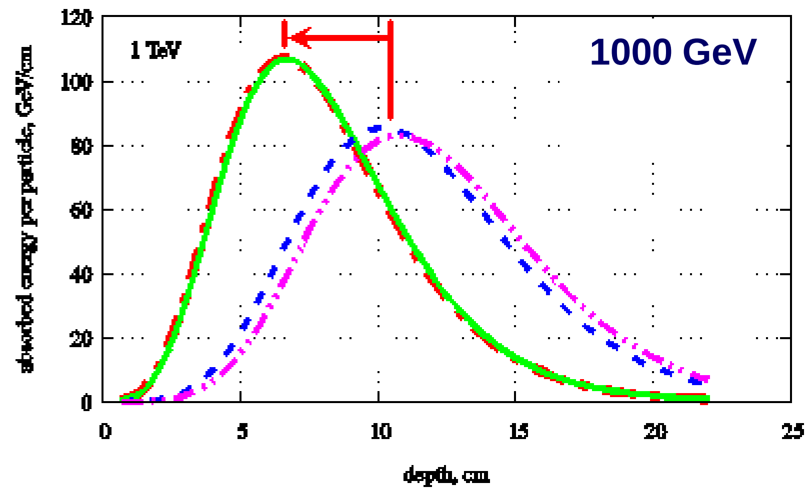

ATLAS collaboration

EUROPEAN ORGANIZATION FOR NUCLEAR RESEARCH (CERN)

CERN-PH-EP/2014-117
2014/07/03

CMS-HIG-13-001

Observation of the diphoton decay of the Higgs boson and measurement of its properties

The CMS Collaboration[*]

Abstract

Observation of the diphoton decay mode of the recently discovered Higgs boson and measurement of some of its properties are reported. The analysis uses the entire dataset collected by the CMS experiment in proton-proton collisions during the 2011 and 2012 LHC running periods. The data samples correspond to integrated luminosities of 5.1 fb^{-1} at $\sqrt{s} = 7$ TeV and 19.7 fb^{-1} at 8 TeV. A clear signal is observed in the diphoton channel at a mass close to 125 GeV with a local significance of 5.7 σ, where a significance of 5.2 σ is expected for the standard model Higgs boson. The mass is measured to be 124.70 ± 0.34 GeV $= 124.70 \pm 0.31$ (stat) ± 0.15 (syst) GeV, and the best-fit signal strength relative to the standard model prediction is $1.14^{+0.26}_{-0.23} = 1.14 \pm 0.21$ (stat) $^{+0.09}_{-0.05}$ (syst) $^{+0.13}_{-0.09}$ (theo). Additional measurements include the signal strength modifiers associated with different production mechanisms, and hypothesis tests between spin-0 and spin-2 models.

Submitted to the European Physical Journal C

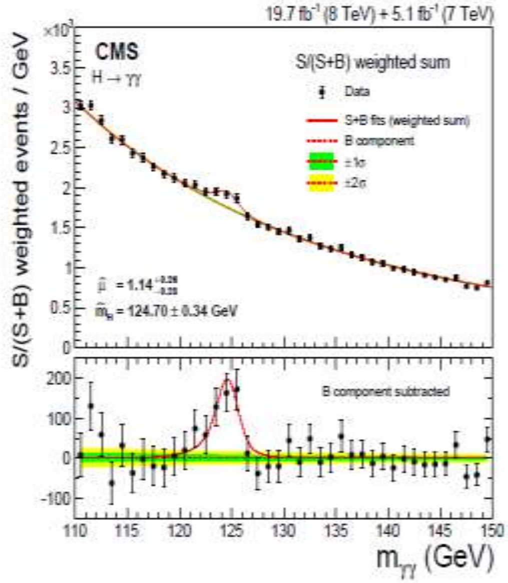

Figure 19: Diphoton mass spectrum weighted by the ratio $S/(S+B)$ in each event class, together with the background subtracted weighted mass spectrum.

Table 5: Values of the best-fit signal strength, $\hat{\mu}$, when m_H is treated as a nuisance parameter, for the 7 TeV, 8 TeV, and combined datasets. The corresponding best-fit value of m_H, $\hat{m}_H$, is also given.

	$\hat{\mu}$	$\hat{m}_H$ (GeV)
7 TeV	$2.22^{+0.62}_{-0.55}$	124.2
8 TeV	$0.90^{+0.26}_{-0.23}$	124.9
Combined	$1.14^{+0.26}_{-0.23}$	124.7

Electromagnetic shower acceleration in PWO can influence H boson mass measurements

ATLAS $m_{H \to \gamma\gamma} = 125.98 \pm 0.50$ GeV

CMS $m_{H \to \gamma\gamma} = 124.70 \pm 0.34$ GeV

Thickness of the CMS ECAL calorimeters can be made smaller

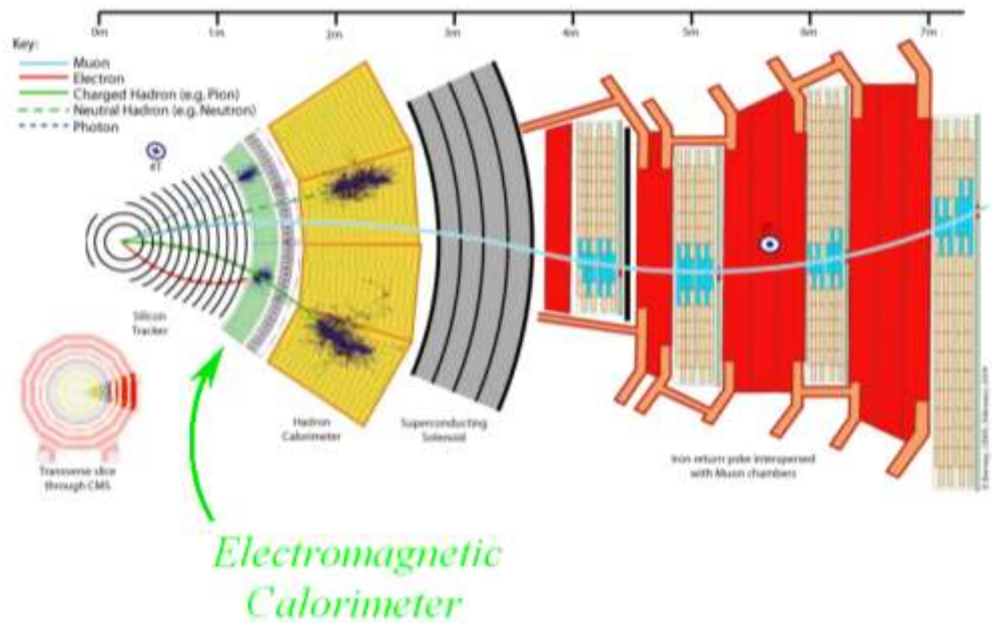

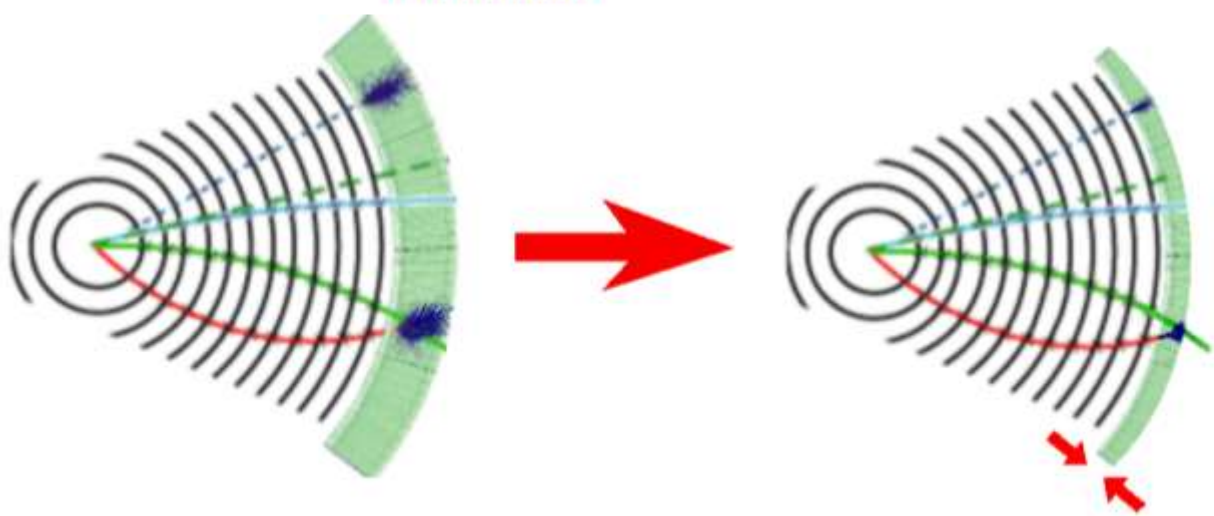

Local secondary particle divergence at the FCC detector is also about 1 **milliradian**

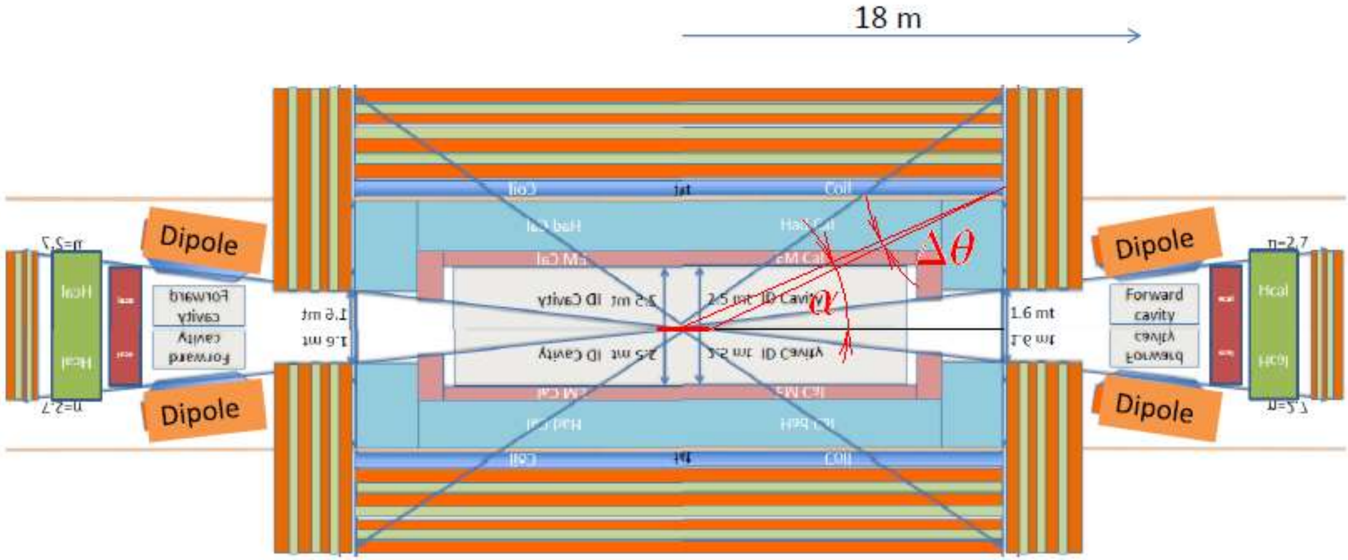

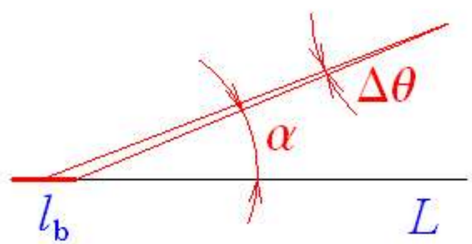

$$\Delta\theta = \frac{l_b}{2L}\cos\alpha\sin\alpha \approx 0.86\,mrad \quad \text{при} \quad \alpha = 20^\circ$$

Positron source for ILC/CLIC

LAL-Orsay, IPNL-Lyon, KEK, Hiroshima University

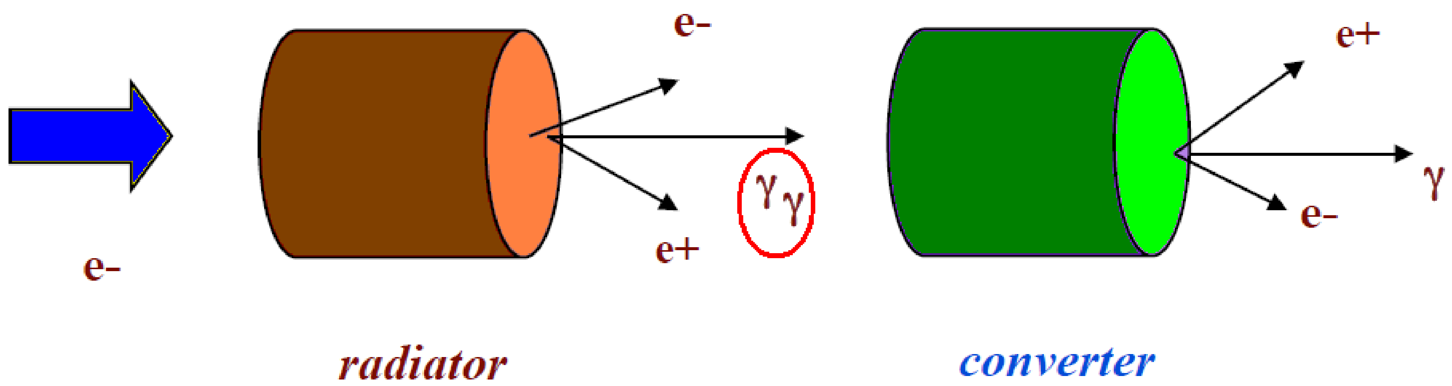

electron radiation in 1 mm W <111>

20 GeV electron trajectory in W<111> 1 mm

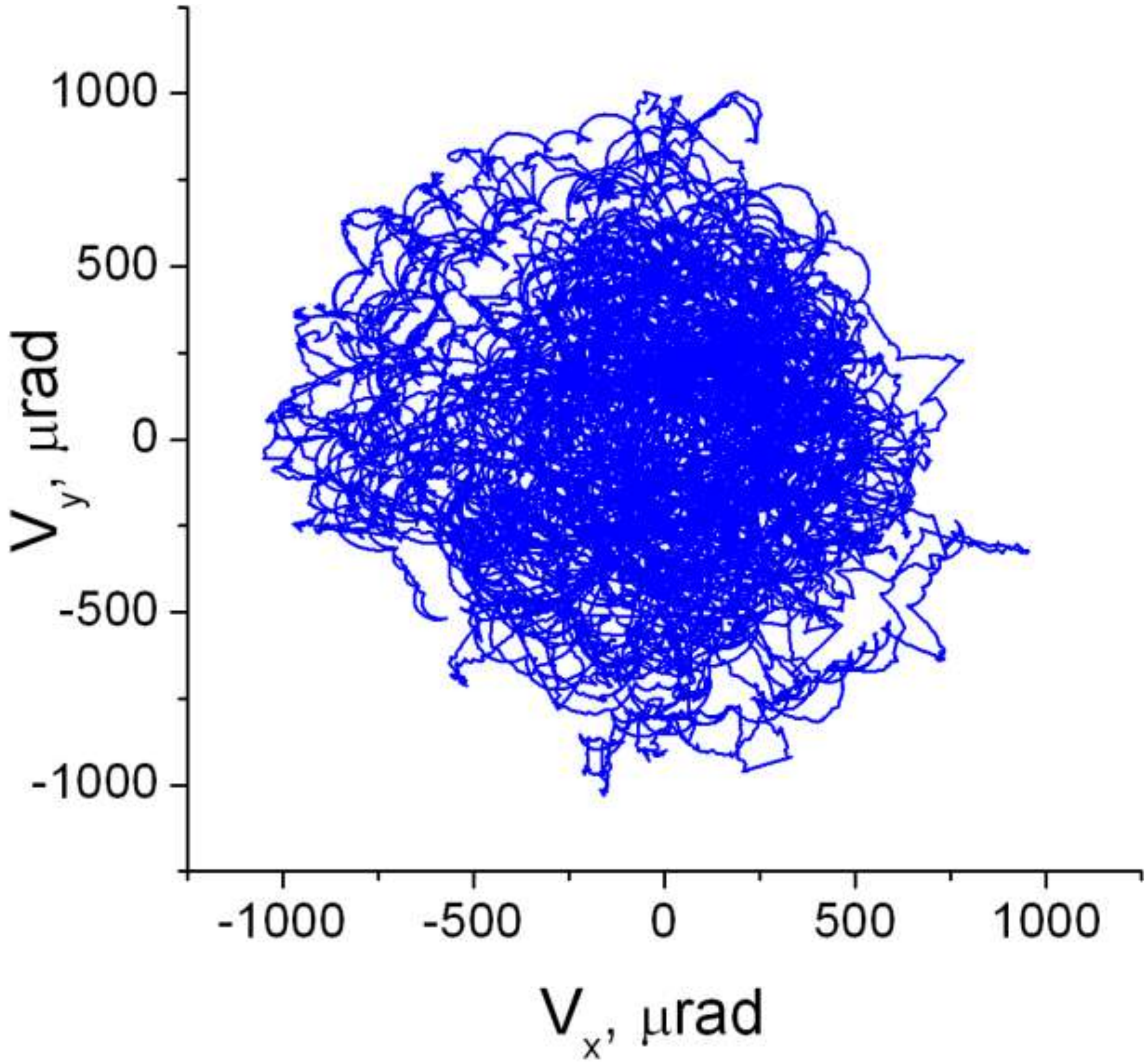

20 GeV **electron** spectrum behind 1 mm <110> W

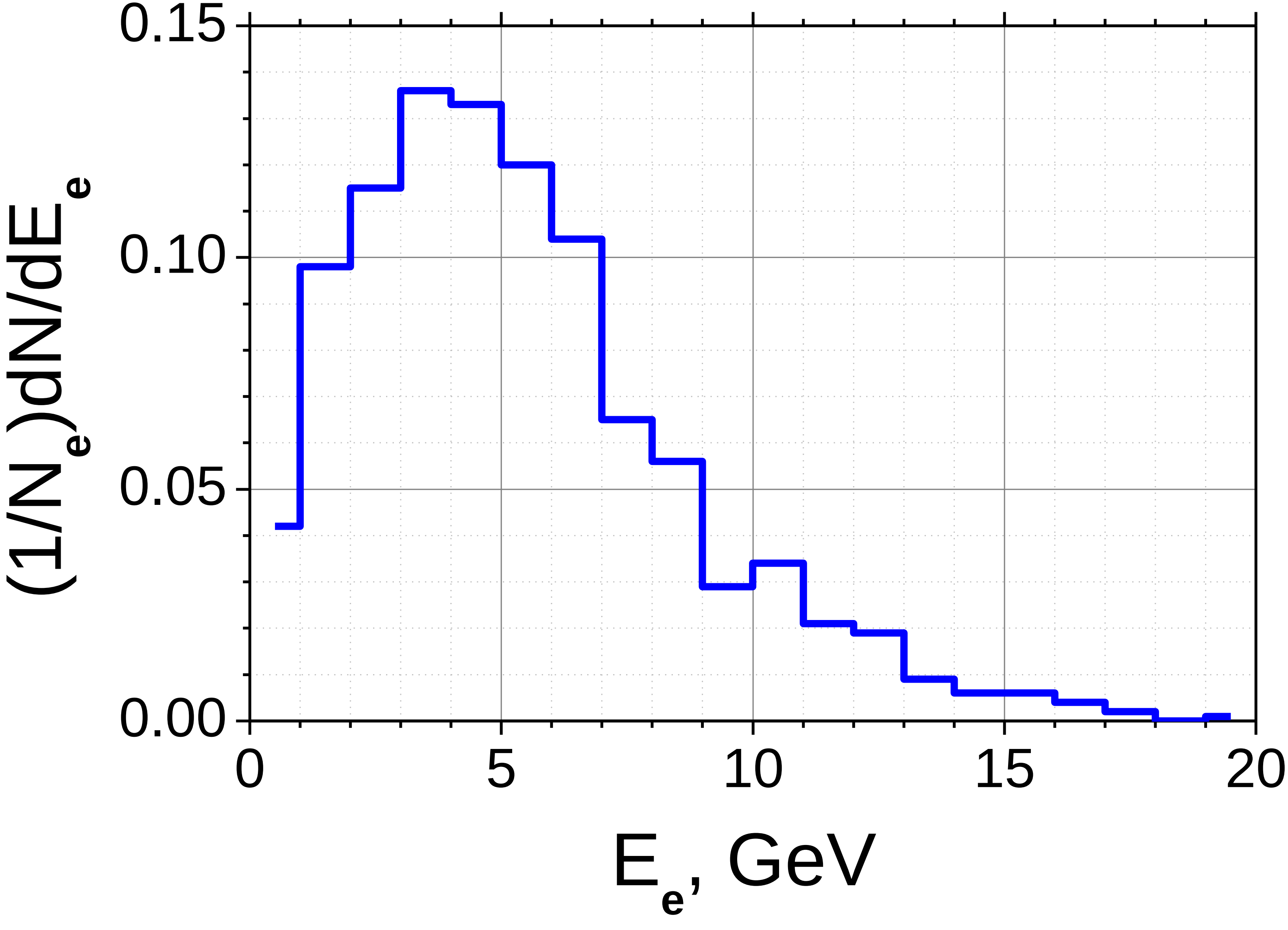

20 GeV e^- radiation amplification in <110> W

1 mm

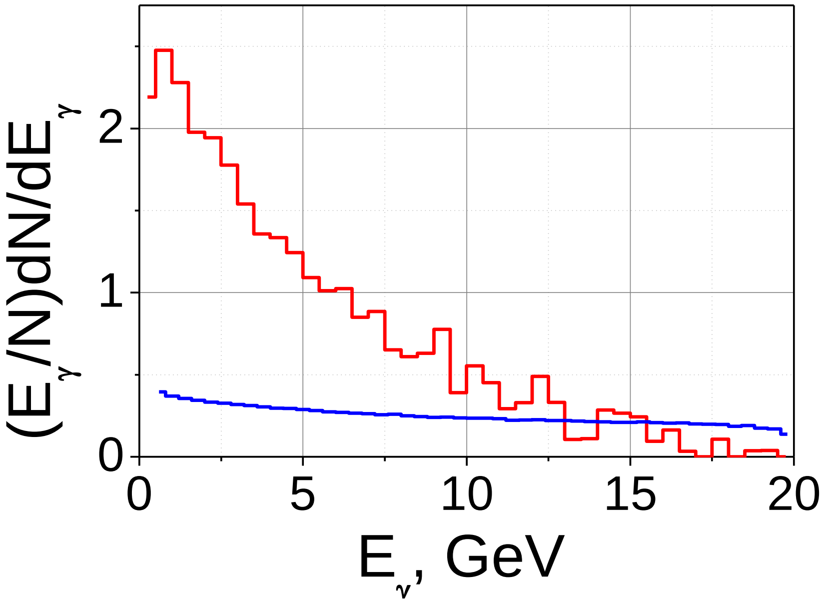

thin (20-30 um)

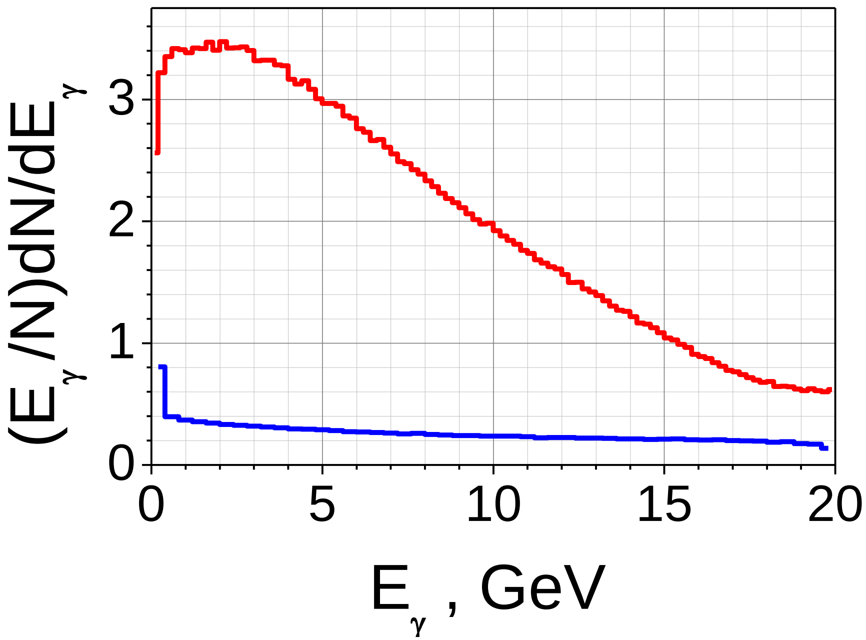

Mind **soft radiation** saturation and suppression!

Special efforts to simulate the soft radiation spectrum part

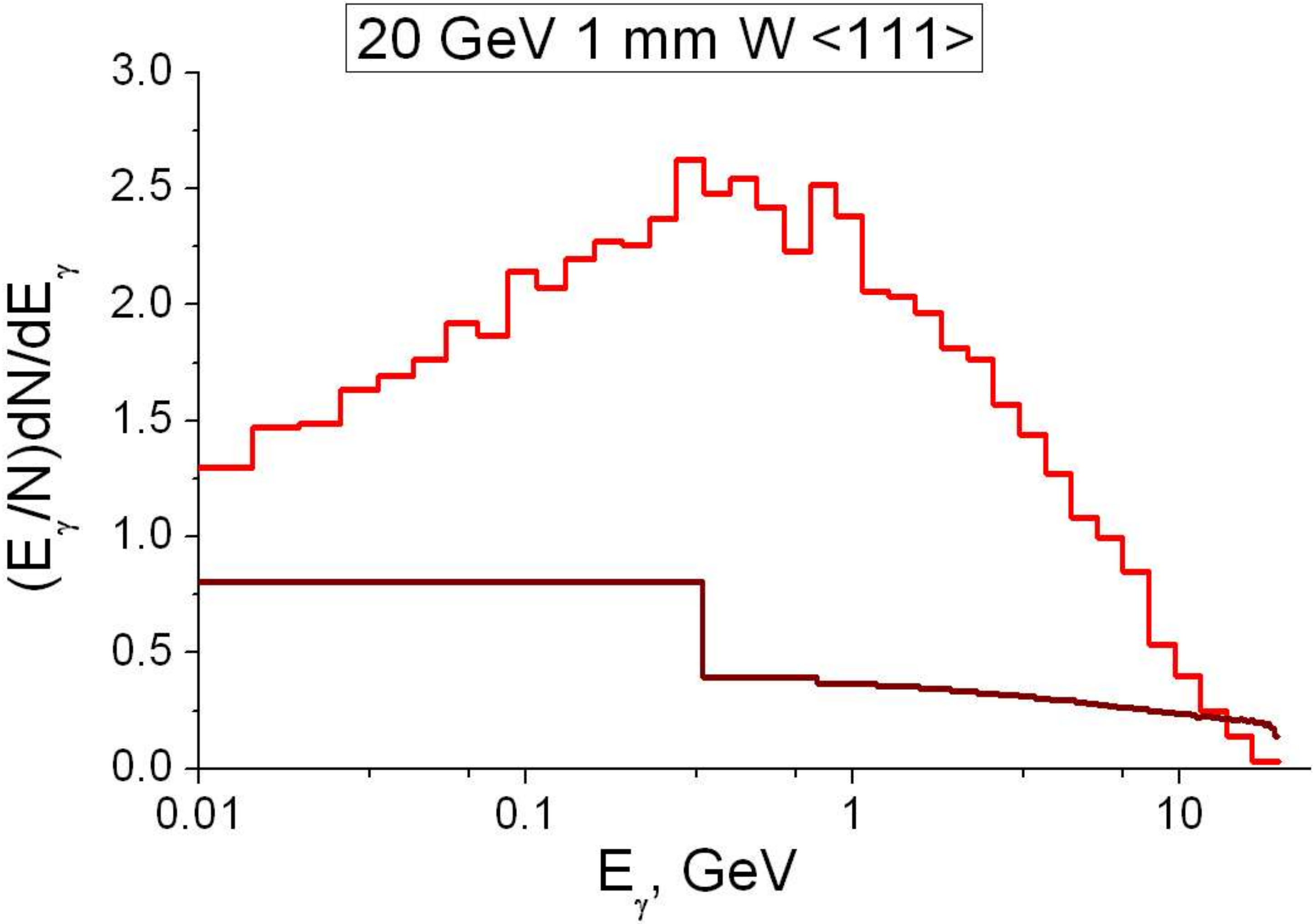

Crystal-based angular-sensitive gamma-telescope

V.A. Baskov, V.A. Khablo, V.V. Kim et al., NIM B 122(1997)194.

V.N. Baier, V.M. Katkov, V.M. Strakhovenko, *Electromagnetic Processes at High Energies in Oriented Single Crystals*, World Scientific, Singapore, 1998.

CsI scintillators
in the **Fermi** Large Aperture Telescope

GLAST Observatory after the integration of the Large Area Space Telescope. Picture taken at the General Dynamic on December 2006.

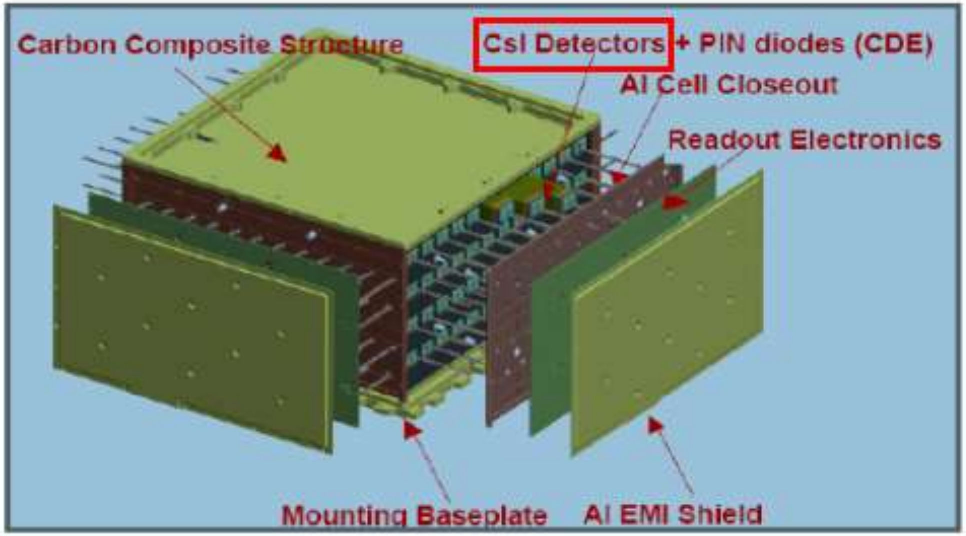

Schematic view of the GLAST imaging calorimeter.

The GAMMA-400 project

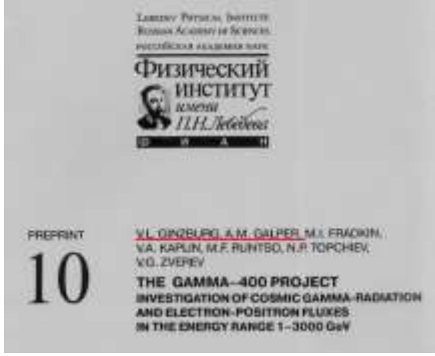

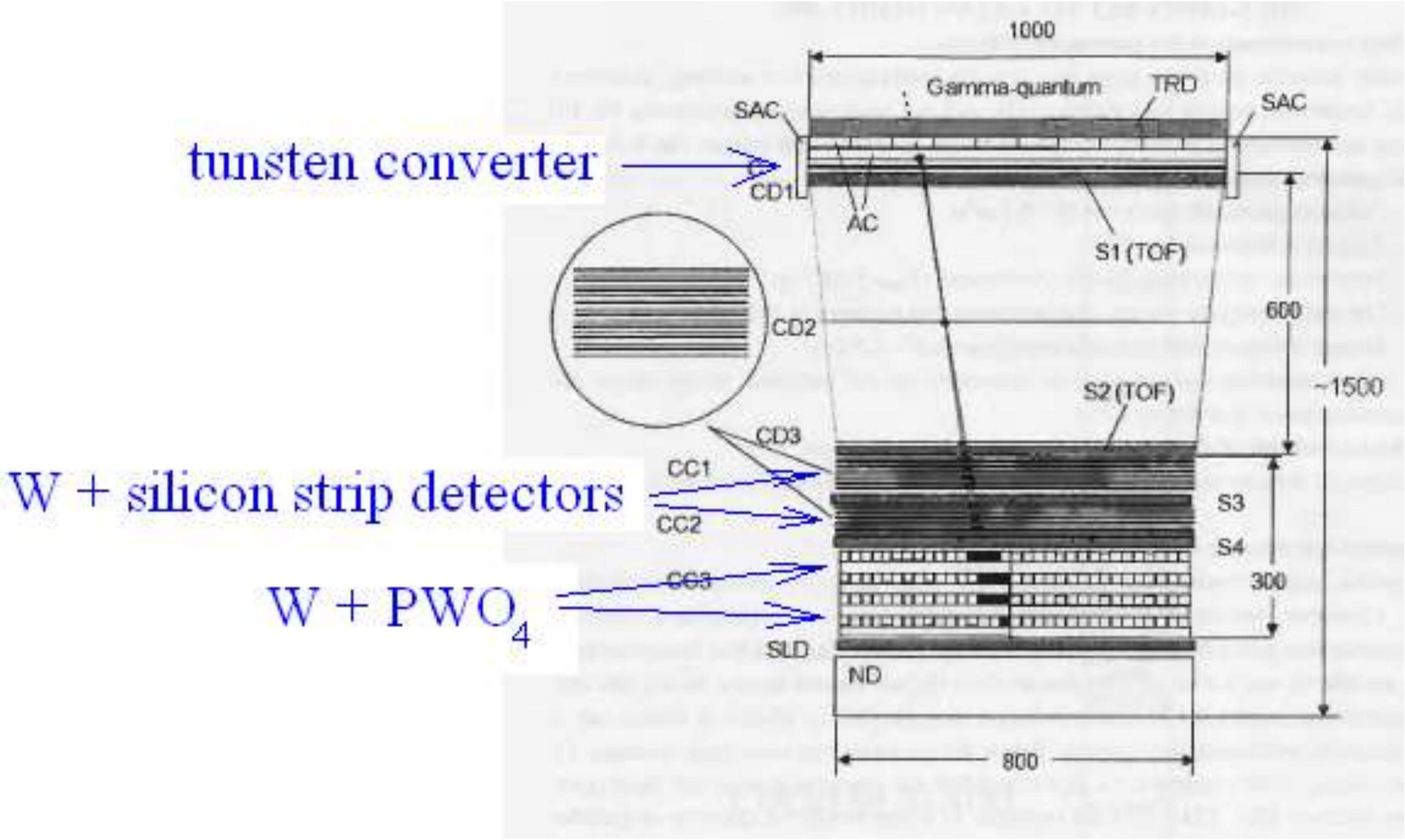

To the crystal gamma-telescope development

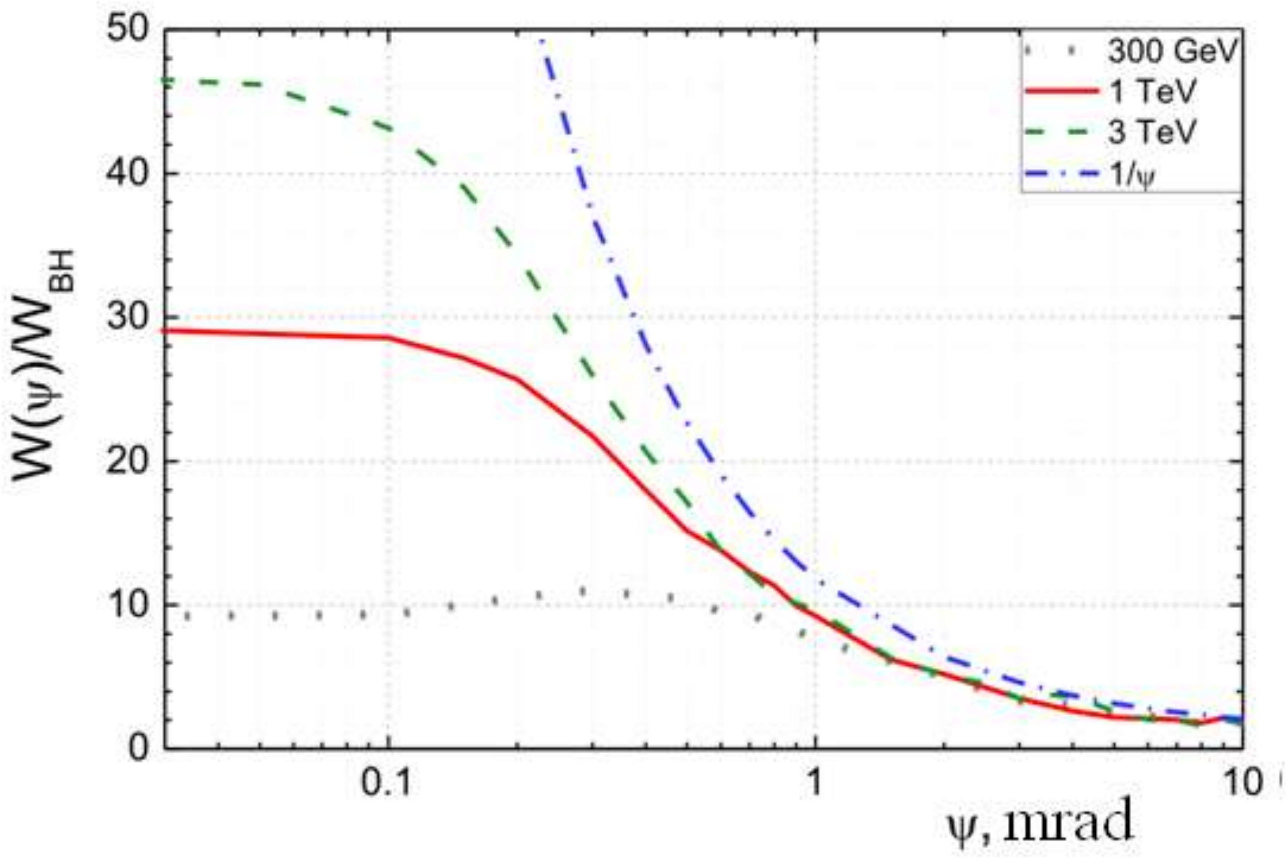

Pair production probability by 300Gev. 1 Tev and 3 TeV gamma-quanta vs the angles of incidence w.r.t. <110> Si axis.

The probability is measured in units of Beth-Heitler PP probability WBH ≈ 0.083/cm.

The averaged field of crystal planes

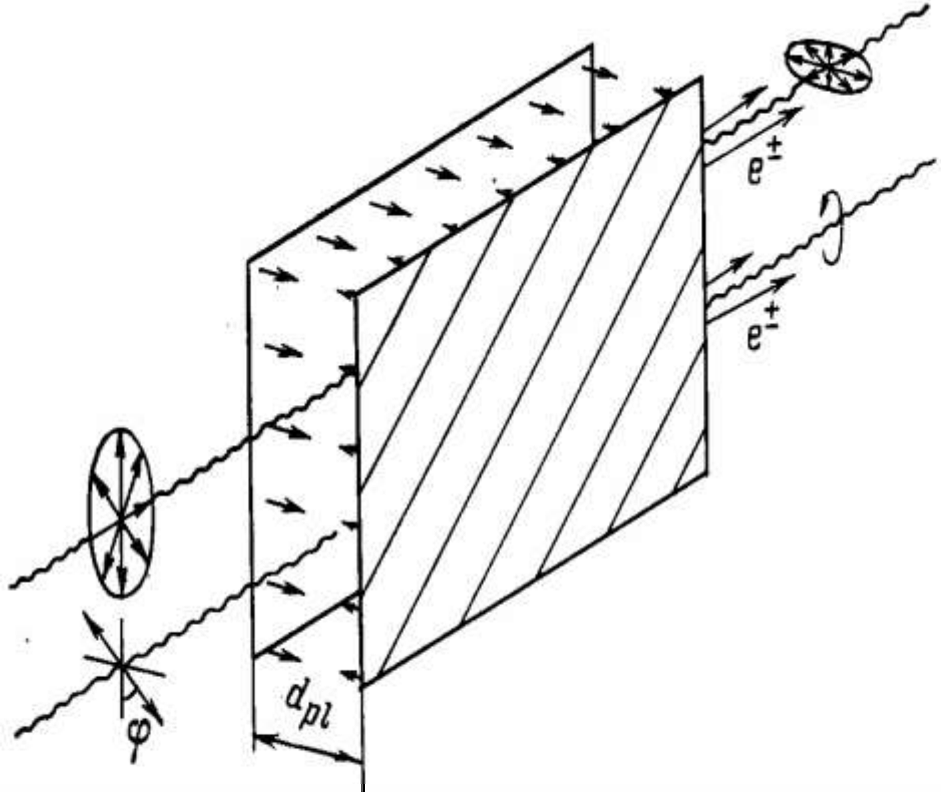

A crystal is *similar* to a region of space occupied by a **uniform electric field** and possesses the properties of **dichroism** *and* **birefringence** in very hard γ -region

Dichroic crystal polarizer

Optimal **polarizer length** and **pair production asymmetry**

Ge crystal (110) plane T=293K

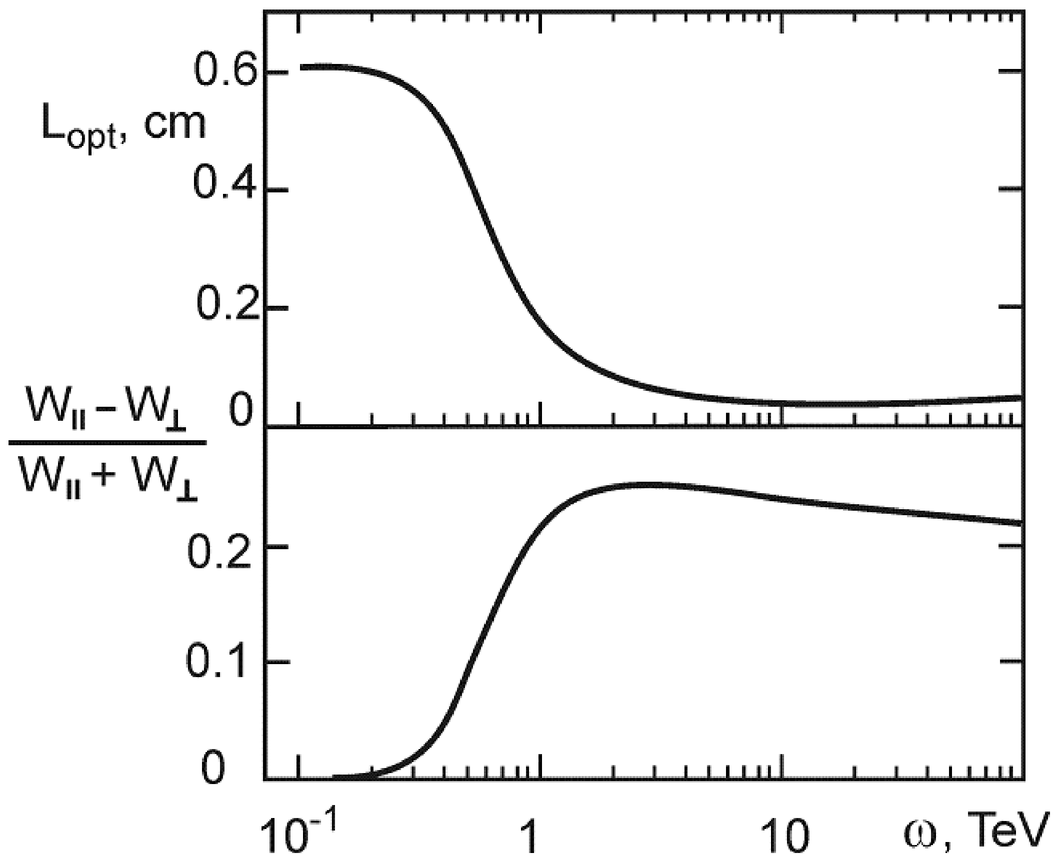

Quarter-wave crystal plate

Energy dependence of **attenuation coefficient** of a completely polarized beam and the **length of quarter-wave plate** based on using the birefringence property of the fields for <110> planes of Si crystal at T=293K

attenuation coefficient

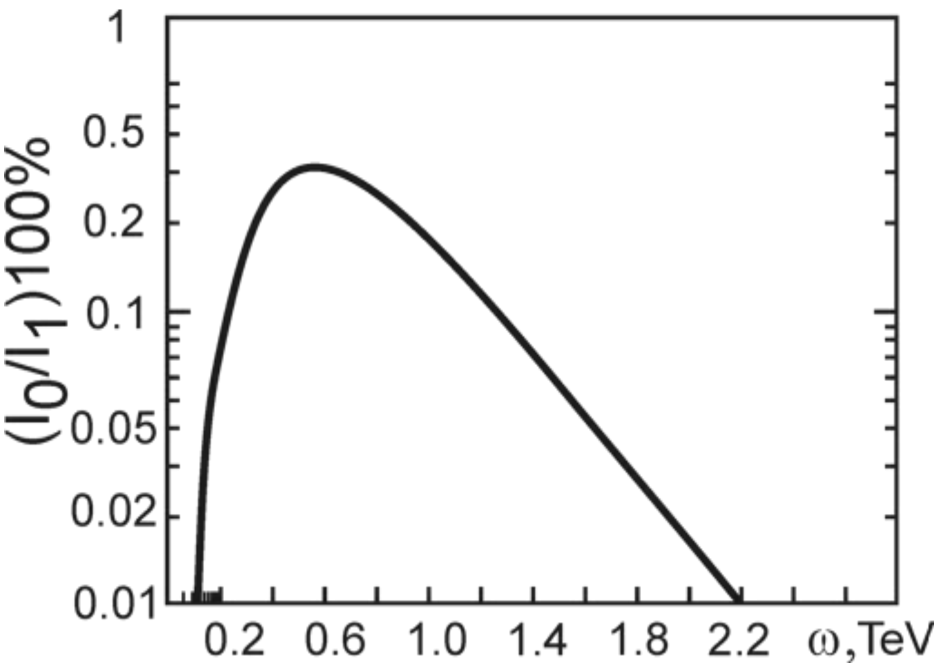

length of quarter-wave plate

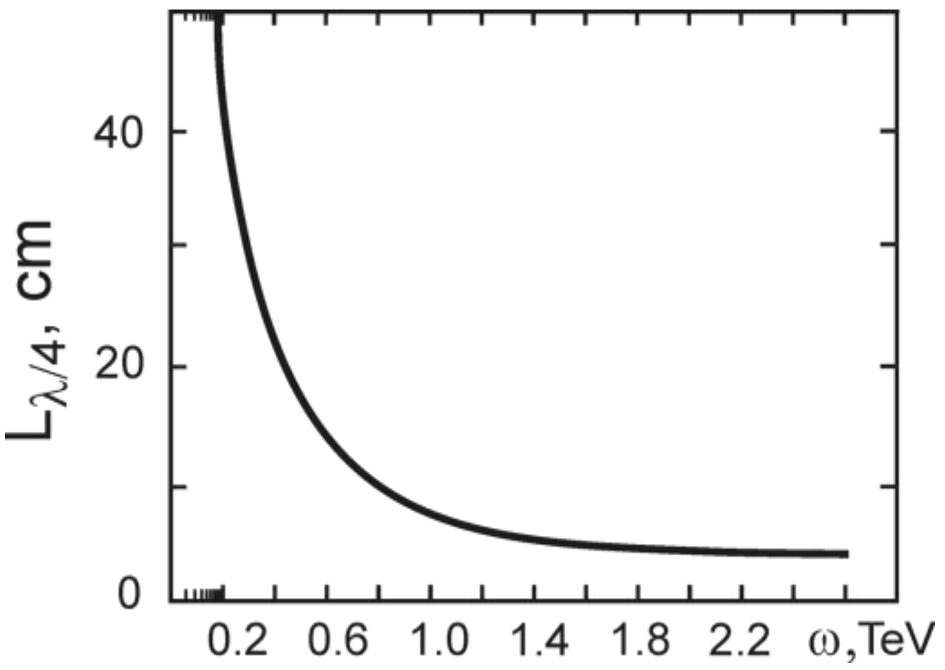

$$L_{\lambda/4}\,\frac{\omega}{c}(n_{\parallel}-n_{\perp})=\frac{\pi}{2}$$

For visible light

$$\Delta t=10^{-15}\,\mathrm{s}$$

For γ - quanta

$$\Delta t=10^{-27}\,\mathrm{s}$$

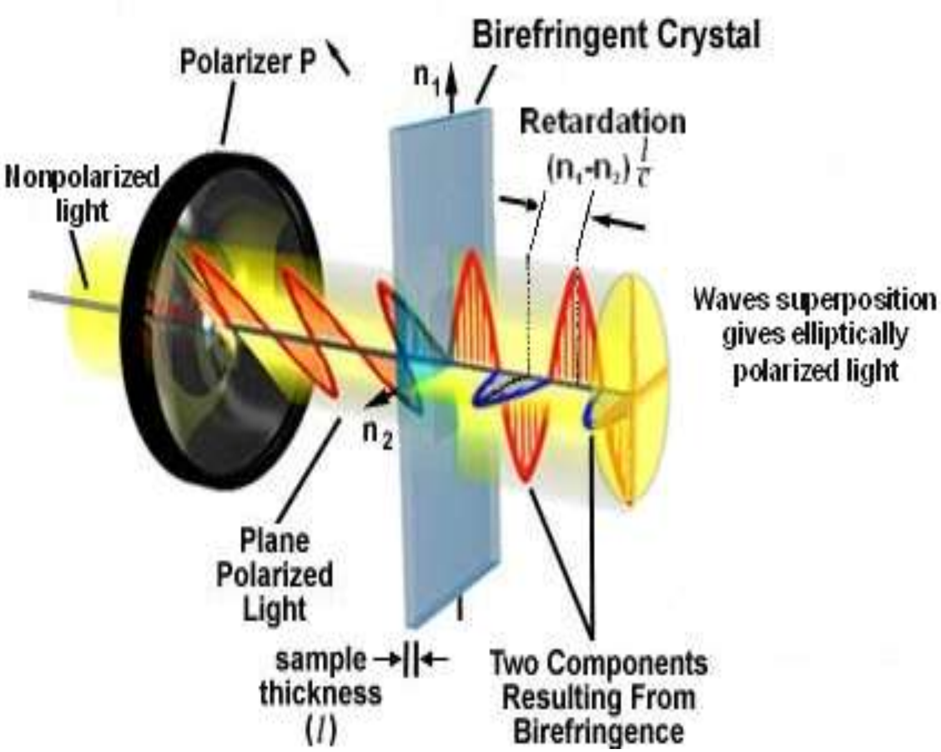

Самое точное измерение возможного нарушения CPT и лоренц-инвариантности

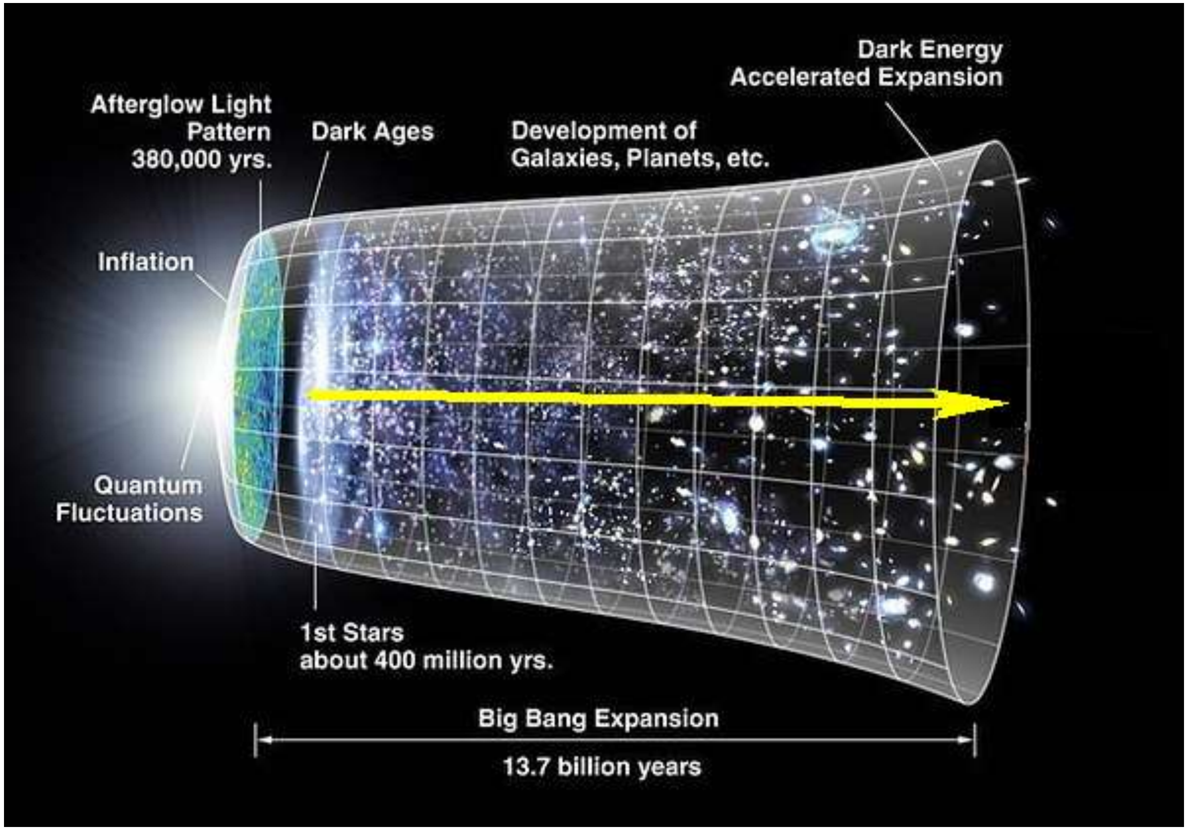

10^{-27} секунд за $13.4 \cdot 10^{9}$ лет $\quad \Delta f / f \sim 10^{-44}$

Most urgent work:

- “innovative” ECALs
- “positron source”
- “innovative” gamma-telescopes
- gamma-flux suppression (CLEVER)
- dark photon search

CMS ECAL ?

GEANT ??

New general simulation tool?

CURRENT WORK DIRECTIONS:

simulation method principles

simulations of

– CU

– PWO, W (“positron source”)

– gamma-telescopes

Thank you for attention!